DMD Fast Forward. Published on February 23, 2017 as DOI: 10.1124/dmd.117.075135
This article has not been copyedited and formatted. The final version may differ from this version.

DMD #75135

RNA-Seq Reveals Age- and Species Differences of CAR-targeted Drug-Processing Genes in Liver

Sunny Lihua Cheng, Theo K. Bammler, and Julia Yue Cui

Laboratories of origin:

SLC, TKB, and JYC: Department of Environmental and Occupational Health Sciences, University of Washington, Seattle 98105

DMD Fast Forward. Published on February 23, 2017 as DOI: 10.1124/dmd.117.075135
This article has not been copyedited and formatted. The final version may differ from this version.

Running title: Regulation of DPGs by CAR in developing liver

Address for correspondence:

Julia Yue Cui, PhD
Assistant Professor
Department of Environmental and Occupational Health Sciences
University of Washington
4225 Roosevelt Way NE, Seattle, WA 98105
Email: juliacui@uw.edu
Tel: 206-616-4331

Document statistics:

Text pages: 38
Tables: 1
Figures: 10
References: 66
Words in Abstract: 264
Words in Introduction: 1051
Words in Discussion: 1476

ABBREVIATIONS

Aadac, arylacetamide deacetylase (esterase); Abc, ATP-binding cassette; Ache, acetylcholinesterase; Acsm, acyl-CoA synthetase medium-chain family member; Adh, alcohol dehydrogenase; Ahr, aryl hydrocarbon receptor; Akr, aldo-keto reductase; Aldh, aldehyde dehydrogenase; Alox5ap, arachidonate 5-lipoxygenase activating protein; Aoc, amine oxidase, copper containing; Aox, aldehyde oxidase; As3mt, arsenic (+3 oxidation state) methyltransferase; Atp7b, ATPase, Cu++ transporting, beta polypeptide; Atp8b1, ATPase, class I, type 8B, member 1; Baat, bile acid-Coenzyme A: amino acid N-acyltransferase; Bche, butyrylcholinesterase; Bphl, biphenyl hydrolase-like (serine hydrolase, breast epithelial mucin-associated antigen); CAR, constitutive androstane receptor; Cbr, carbonyl reductase; Ces, carboxyesterase; CITCO, 6-(4-Chlorophenyl)imidazo[2,1-b][1,3]thiazole-5-carbaldehyde O-(3,4-dichlorobenzyl)oxime; Comt, catechol-O-methyltransferase; Cyp, cytochrome P450; Dao, D-amino acid oxidase; Dhdh, dihydrodiol dehydrogenase (dimeric); Dhrs,

dehydrogenase/reductase (SDR family); DPG, drug-processing gene; Dpyd, dihydropyrimidine dehydrogenase; Ephx, epoxide hydrolase; Epx, eosinophil peroxidase; Esd, esterase D/formylglutathione hydrolase; Fmo, flavin containing monooxygenase; FXR, farnesoid X receptor; Gamt, guanidinoacetate methyltransferase; Gclc, glutamate-cysteine ligase, catalytic subunit; Gclm, glutamate-cysteine ligase, modifier subunit; Glrx, glutaredoxin; Glyat, glycine-N-acyltransferase; Gnmt, glycine N-methyltransferase; Gphn, gephyrin; Gpx, glutathione peroxidase; Gsr, glutathione reductase; Gst, glutathione S-transferase; Gusb, glucuronidase, beta; Hnmt, histamine N-methyltransferase; Hpgds, hematopoietic prostaglandin D synthase; Inmt, indolethylamine N-methyltransferase; Lcat, lecithin cholesterol acyltransferase; Lipa, lysosomal acid lipase A; Lox, lysyl oxidase; Lpo, lactoperoxidase; Lta4h, leukotriene A4 hydrolase; Ltc4s, leukotriene C4 synthase; Mao, monoamine oxidase; Mocos, molybdenum cofactor sulfurase; Mocs, molybdenum cofactor synthesis; Mpo, myeloperoxidase; mRNA, messenger RNA; Nat, N-acetyltransferase; Nnmt, nicotinamide N-methyltransferase; Nqo, NAD(P)H dehydrogenase, quinone; Paox, polyamine oxidase (exo-N4-amino); Papss, 3'-phosphoadenosine 5'-phosphosulfate synthase; Pemt, phosphatidylethanolamine N-methyltransferase; Pnmt, phenylethanolamine-N-methyltransferase; Pon, paraoxonase; Por, P450 (cytochrome) oxidoreductase; Prdx, peroxiredoxin; Ptges, prostaglandin E synthase; Ptgs, prostaglandin-endoperoxide synthase; PXR, pregnane X receptor; RNA-Seq, RNA sequencing; SAM, Sequence Alignment/Map; Sars, seryl-aminoacyl-tRNA synthetase; Sdr, short chain dehydrogenase/reductase family; Slc, solute carrier family; Slco, solute carrier organic anion transporter family; Smox, spermine oxidase; Soat1, sterol O-acyltransferase; Sult, sulfotransferase; Suox, sulfite oxidase; TCPOBOP, 1,4-Bis-[2-(3,5-dichloropyridyloxy)]benzene, 3,3′,5,5′-Tetrachloro-1,4-bis(pyridyloxy)benzene; Tpmt, thiopurine methyltransferase; Tpo, thyroid peroxidase; Txn, thioredoxin; Txnrd, thioredoxin reductase; Ugdh, UDP-glucose dehydrogenase; Ugp2, UDP-glucose pyrophosphorylase 2; Ugt, UDP glucuronosyltransferase; Xdh, xanthine dehydrogenase.

DMD Fast Forward. Published on February 23, 2017 as DOI: 10.1124/dmd.117.075135
This article has not been copyedited and formatted. The final version may differ from this version.

ABSTRACT

The constitutive androstane receptor (CAR/Nr1i3) is an important xenobiotic-sensing nuclear receptor that is highly expressed in liver, and is well known to have species differences. During development, age-specific activation of CAR may lead to modified pharmacokinetics and toxicokinetics of drugs and environmental chemicals, leading to higher risks for adverse drug reactions in newborns and children. The goal of this study was to systematically investigate the age- and species-specific regulation of various drug-processing genes following neonatal or adult CAR activation in livers of wild-type (WT), CAR-null, and humanized CAR-transgenic (hCAR-TG) mice. At either 5- or 60-days of age, the 3 genotypes of mice were administered a species-appropriate CAR ligand or vehicle once daily for 4-days (i.p.). The majority of DPGs were differentially regulated by age and/or CAR activation. There were 36 DPGs that were commonly up-regulated by CAR activation regardless of age or species of CAR. Although the cumulative mRNAs of uptake transporters were not readily altered by CAR, the cumulative Phase-I and –II enzymes as well as efflux transporters were all increased following CAR activation in both species. In general, mCAR activation produced comparable or even greater fold-increases of many DPGs in newborns than in adults; conversely, hCAR activation produced weaker induction in newborns than in adults. Western blotting and enzyme activity assays confirmed the age- and species-specificities of selected CAR-targeted DPGs. In conclusion, the present study has systematically compared the effect of age and species of CAR proteins on the regulation of DPGs in liver, and has demonstrated that the regulation of xenobiotic biotransformation by CAR is profoundly modified by age and species.

DMD Fast Forward. Published on February 23, 2017 as DOI: 10.1124/dmd.117.075135
This article has not been copyedited and formatted. The final version may differ from this version.

INTRODUCTION

Liver is a major organ for the biotransformation of various drugs and environmental chemicals. In hepatocytes, many Phase-I and Phase-II drug-metabolizing enzymes as well as uptake and efflux transporters (together called DPGs) are highly expressed (Almazroo et al., 2017; Klaassen and Aleksunes, 2010; Fu et al., 2016). Xenobiotics are taken up into the hepatocytes by various uptake transporters in the solute carrier (Slc and Slco) family (Klaassen and Aleksunes, 2010), and where they are frequently modified by various Phase-I enzymes including those that catalyze 1) oxidation reactions such as cytochrome P450s (Cyps), alcohol dehydrogenases (Adhs), aldehyde dehydrogenase (Aldh), molybdenum hydroxylases, aldehyde oxidases, dimeric dihydrodiol dehydrogenases, amine oxidases, flavin monooxygenases (Fmos), and peroxidases; 2) reduction reactions such as azo- and nitro-reduction, carbonyl reduction, disulfide reduction, sulfoxide reduction, quinone reduction (by NAD(P)H, quinone oxidoreductases (Nqos), dehalogenation, and dehydroxylation; and 3) hydrolysis reactions as catalyzed by carboxyesterases (Cess), cholinesterases, paraoxonases (Pons), epoxide hydrolases (Ephx), peptidases, and β-glucuronidases (Parkinson et al., 2013; Cui and Li, 2016). Phase-II reactions including glucuronidation (by UDP-glucuronosyltransferases [Ugts]), sulfonation (by sulfotransferases [Sults]), glutathione conjugation (by glutathione-*S*-transferases [Gsts]), and amino acid conjugation (by various enzymes such as medium-chain CoA ligases, acyl-CoA: glycine *N*-acetyltransferases, seryl-tRNA synthetases, and bile acid conjugation enzymes), increase the water solubility of the substrates and favor their excretion. Whereas other Phase-II reactions including acetylation (by *N*-acetyl transferases [Nats]), methylation (by various methyltransferases), and fatty acid conjugation (by acyltransferases and cholesterol ester hydrolases) result in decreased water solubility of the substrates (Parkinson et al., 2013; Cui and Li, 2016). Many conjugated metabolites are substrates for efflux transporters in the

ATP-binding cassette (ABC) family and some solute carrier families (Klaassen and Aleksunes, 2010).

The nuclear receptor CAR is an important xenobiotic-sensing transcription factor that is highly expressed in liver (Bookout et al., 2006; Yan and Xie, 2016). The prototypical CAR activator is the anticonvulsant phenobarbital (indirect activator) in both rodents and humans, 1,4-bis-[2-(3,5- dichloropyridyloxy)]benzene,3,3′,5,5′-tetrachloro-1,4-bis(pyridyloxy)benzene (TCPOBOP, direct ligand) in rodents only (Tzameli et al., 2000), as well as 6-(4-chlorophenyl)imidazo[2,1-b][1,3]thiazole-5-carbaldehyde-O-(3,4-dichlorobenzyl)oxime (CITCO, direct ligand) in humans only (Maglich et al., 2003; Windshugel and Poso, 2011). Upon activation, it is well known that CAR up-regulates the expression of a wide-spectrum of DPGs in adult livers and in liver-derived cell culture in a CAR-dependent manner (Wortham et al., 2007; Aleksunes and Klaassen, 2012; Li et al., 2015; Cui and Klaassen, 2016). In addition to the prototypical CAR activators, many other human-relevant xenobiotics such as certain herbal medicines and environmental chemicals can also activate CAR (Huang et al., 2004; Ross et al., 2010; Sueyoshi et al., 2014; Zhang et al., 2015). Therefore, CAR is partially involved in adverse drug reactions. One potential problem of investigating CAR in animal models is the species-differences between CAR proteins in humans and rodents (Holsapple et al., 2006; Ross et al., 2010; Yang and Wang, 2014). For example, mCAR activation promotes tumor in liver (Yamamoto et al., 2004; Huang et al., 2005); conversely, hCAR activation is associated with cell cycle arrest and enhanced apoptosis, suggesting an anti-cancer potential (Chakraborty et al., 2011). Although it is generally recognized that CAR is important in regulating drug metabolism and transport in livers of both species, there have been no systematic studies specifically comparing the effects of CAR activation on all the hepatic DPG expression between mice and humans. Human livers and *in vitro* human primary hepatocyte culture are the gold standards to investigate the effect of CAR activation in humans. However, these approaches are limited by

DMD Fast Forward. Published on February 23, 2017 as DOI: 10.1124/dmd.117.075135
This article has not been copyedited and formatted. The final version may differ from this version.

scarcity of sources, large biological and/or technical variations, and ethical concerns. To understand the species differences in CAR-mediated regulation of hepatic target genes *in vivo*, various humanized CAR-transgenic (hCAR-TG) mice have been generated (Scheer et al., 2008; Zhang et al., 2013). The hCAR-TG mice utilized in the present study not only include the exons and promoters, but also 73-kb upstream and 91-kb downstream regulatory DNA into the mouse genome utilizing the BAC-transgenic technology, allowing the investigation of the regulation of CAR-target genes as well as the transcription of CAR itself (Zhang et al., 2013). This hCAR-TG mouse model expresses major *hCAR* SVs in humans, and it is functional in terms of up-regulating the prototypical CAR-target gene Cyp2b10 (which is the human CYP2B6 homolog), allowing an *in vivo* investigation on hCAR function in response to chemical activation.

Another important yet under-studied area is the chemical-mediated regulation of CAR-targeted genes during development. At birth, profound changes occur in liver transitioning from a hematopoietic organ to the major organ for xenobiotic biotransformation. Although the basal ontogenic expression of various DPGs has been characterized in wild-type mouse livers (O'Sullivan et al., 1989; Cui et al., 2010; Cui et al., 2012a; Peng et al., 2012; Lu et al., 2013; Peng et al., 2013; Gunewardena et al., 2015) and in human liver samples (Hines and McCarver, 2002; McCarver and Hines, 2002; Hines, 2007; Hines, 2013; Mooij et al., 2014; Mooij et al., 2016; Thomson et al., 2016), very little is known regarding the age-specific transcriptional responses of the hepatic DPGs following exposure to foreign chemicals such as therapeutic drugs, dietary factors, and environmental toxicants (Lee et al., 2008; Xiao et al., 2012). Age-specific expression of chromatin epigenetic marks in liver suggests that the accessibility of transcription factors to target genes in the genome and the subsequent changes in target-gene expression are highly regulated by age (Lu et al., 2012). Among various xenobiotics to which pediatric patients are exposed, a considerable portion may activate the CAR receptor (Huang et al., 2004; Ross et al., 2010; Sueyoshi et al., 2014; Zhang et al., 2015), placing newborns and children at a higher risk for adverse drug reactions and chemical-induced liver injuries.

DMD Fast Forward. Published on February 23, 2017 as DOI: 10.1124/dmd.117.075135
This article has not been copyedited and formatted. The final version may differ from this version.

Neonatal activation of mCAR in mouse liver leads to persistent increase in certain drug-metabolizing enzymes in liver in adult age (Chen et al., 2012; Li et al., 2016a), however, there have been no systematic studies conducted to determine to what extent the acute pharmacological activation of CAR leads to age- and species-specific regulation of hepatic DPGs.

Therefore, the purpose of this study was to use RNA-Seq to systematically characterize and compare the regulation of DPGs by CAR in an age- and species-specific manner, using WT, hCAR-TG, and CAR-null mice in neonatal and adult ages. The selection of 393 important DPGs was based on previous studies in the literature (Parkinson et al., 2013; Cui and Li, 2016).

MATERIALS AND METHODS

Chemicals and Reagents

Corn Oil, TCPOBOP, and CITCO were purchased from Sigma Aldrich (St. Louis, MO). Liquid alanine aminotransferase (ALT) assay kit was purchased from Pointe Scientific Inc. (Canton, MI). RNA-Bee reagent was purchased from Tel-Test Inc. (Friendswood, TX). The primers were designed using Primer3 (http://bioinfo.ut.ee/primer3-0.4.0/) and were purchased from Integrated DNA Technologies (Coralville, IA). The High-capacity cDNA Reverse Transcription kits, Power SYBR Green PCR Master Mix, Bolt® 4-12% Bis-Tris Plus Gel, Bolt antioxidant, 10X PBS buffer PH 7.4, and UltraPure™ DNase/RNase-free distilled water were purchased from Life Technologies (Carlsbad, CA). The P450-Glo™ screening systems for CYP1A2, CYP2B6, CYP3A4 and the NADPH Regeneration System were purchased from Promega (Madison, WA).

Animal procedures

The university of Washington Office of Animal Welfare approved all experiments. Eight-week-old male C57BL/6J mouse breeders were purchased from the Jackson Laboratory (Bar Harbor,

DMD Fast Forward. Published on February 23, 2017 as DOI: 10.1124/dmd.117.075135
This article has not been copyedited and formatted. The final version may differ from this version.

ME). Breeders of the CAR-null mice in the C57BL/6 background were obtained from Amgen (Thousand Oaks, CA). Breeders of the hCAR-TG mice in the C57BL/6 background were provided from the University of Kansas Medical Center (Kansas City, KS) (Zhang and Klaassen, 2013). Mice were housed and bred according to the standard conditions in the animal facilities of the University of Washington as described by the American Animal Association Laboratory Animal Care Guidelines. All animals were given *ad libitum* access to purified water and irradiated Picolab Rodent Diet 20 number 5053 (PMI Nutrition International, Brentwood, MO), and were housed under a relative humility of 40-60% and on a 12-hour light-dark circle. Mice were randomly assigned to various treatment groups. To avoid variations due to the estrous cycle, only male pups were used in the present study. A dose-response of TCPOBOP and CITCO was performed at 5-day-old neonatal age, whereas a single optimal dose was selected at 60-day-old adult age based on the literature. As described in Figure 1A, at 5-day-old neonatal age, WT and CAR-null mice were administered various doses of the mCAR ligand TCPOBOP (0.3 mg/kg, 1 mg/kg, 3 mg/kg, i.p.) or vehicle (corn oil, 10 ml/kg, i.p.); whereas the hCAR-TG mice were administered various doses of the hCAR ligand CITCO (2.5 mg/kg, 10 mg/kg, 30 mg/kg, i.p.) or vehicle (corn oil, 10 ml/kg, i.p.), once daily for 4 consecutive days (n=5 per group). At 60-day-old adult age, WT and CAR-null mice were administered the mCAR ligand TCPOBOP (3 mg/kg, i.p.) or vehicle (corn oil, 10 ml/kg, i.p.), whereas the hCAR-TG mice were administered the hCAR ligand CITCO (30 mg/kg, i.p.) or vehicle (corn oil, 10 ml/kg, i.p) once daily for 4 consecutive days (n=5 per group). Livers were removed 24-hours after the final dose, immediately frozen in liquid nitrogen, and stored at -80 °C until further analysis.

RNA isolation

Total RNA was isolated from livers of WT, CAR-null and hCAR-TG mice using the RNA-Bee Reagent (Tel-test Inc. Friendswood, TX) following the manufacturer´s instructions. RNA was dissolved in DNase/RNase-free water, and the concentrations were determined

spectrophotometrically at 260 nm using a Nano-Drop 1000 spectrophotometer (Thermo Scientific, Waltham, MA). The integrity of the total RNA was evaluated using an Agilent 2100 Bioanalyzer (Agilent Technologies Inc., Santa Clara, CA). Samples with RNA integrity values larger than 8.0 were used for further analysis.

RT-qPCR Analysis

The total RNA samples were reverse transcribed into cDNAs using a High Capacity cDNA kit (Life Technologies, Carlsbad, CA) according to the manufacture´s instructions. Quantitative real-time PCR assay was performed using a Power SYBR Green PCR Master Mix (Life Technologies, Carlsbad, CA) under a Bio-rad CFX384 Real-Time Detection system (Bio-Rad, Hercules, CA). The primer sequences for real-time PCR reactions were listed in Supplemental Table 3. Expression values were analyzed by the following equation: Relative % = 2^{-dCt} target gene /2^{-dCt} β-actin ×100%, where dCt represents the differences in the cycle threshold numbers between each of the target gene and the reference gene average.

cDNA library construction and RNA sequencing

Three representative liver samples from WT (Corn Oil and TCPOBOP treated) and hCAR-TG mice (Corn Oil and CITCO treated) were selected for RNA sequencing at the University of Washington Genome Sciences Sequencing Facilities. The cDNA libraries from all samples were prepared from 1.25 μg of total RNA in an automated and high-throughput format using the TruSeq Stranded mRNA kit (Illumina, San Diego, CA). All steps required for the sequence library construction were performed in an automated workflow on a Sciclone NGSx Workstation (Perkin Elmer, Waltham, MA). During library construction, ribosomal RNA was depleted by means of a poly-A enrichment. RNA fragmentation, first and second strand cDNA syntheses were performed, and each library was technically barcoded using the Illumina adapters and amplified using a total of 13 cycles of PCR. After amplification and cleanup, library concentrations were quantified using the Quant-it dsDNA Assay (Life Technologies, Carlsbad,

CA). Libraries were subsequently normalized and pooled based on the Agilent 2100 Bioanalyzer results. Sequencing was performed on an Illumina HiSeq 2000 sequencer using a 50 bp paired-end multiplexing strategy with 5 samples per lane.

RNA sequencing data analysis

After the sequencing images were generated by the sequencing platform, the raw data collection, image analysis, and base calls were generated in Illiumina Real Time Analysis (RTA) software. Illumina RTA-output base calling (BCL) files were converted to qseq files using the Illumina BCL Converter software and were subsequently converted to FASTQ files for downstream analysis. Custom scripts developed in-house were used to process the FASTQ files and to output de-multiplexed FASTQ files by lane and index sequence. The quality of the reads was examined using the FASTX-toolkit (http://hannonlab.cshl.edu/fastx_toolkit/) and FastQC (http://www.bioinformatics.babraham.ac.uk/projects/fastqc/). RNA-sequencing reads from the FASTQ files were mapped to the UCSC mm10 mouse reference genome using HISAT (Daehwan Kim et al., 2015). Aligned data were sorted and converted to BAM format using Samtools (version 0.1.9), and then Cufflinks (version 2.2.1) was used for isoform assembly and quantitation analysis. The mRNA abundance was expressed as fragments per kilobase of exons per million reads mapped (FPKM). Differential expression analysis was performed using Cuffdiff (FDR-BH < 0.05).

Western blot analysis

Liver samples were weighed and transferred into a Dounce Homogenizer with 5 volumes (w/v) of ST buffer (10 mM Tris base, 250 mM sucrose, pH 7.5) containing a protease inhibitor cocktail (1:200) (Sigma-Aldrich Corp., St. Louis, MO). The livers were homogenized in an ice-cold condition, and then transferred to Polycarbonate tubes (Beckman Coulter Inc., USA). The crude membranes were prepared by ultra-speed centrifugation of the liver homogenates at 10,000 g for 10 min at 4 °C using an L8-70 M Ultra centrifuge (Beckman, USA). The protein

DMD Fast Forward. Published on February 23, 2017 as DOI: 10.1124/dmd.117.075135
This article has not been copyedited and formatted. The final version may differ from this version.

concentrations were determined using a Qubit Protein Assay Kit (Life Technologies, Carlsbad, CA) per the manufacturer's instructions. Equal amount of protein samples with loading buffer were loaded and electrophoretically separated on a NuPAGE Novex 4-12% Bis-Tris gel, and then transferred onto a polyvinylidene difluoride (PVDF) blotting membrane at 20 V for 5 hours. Subsequently, membranes were blocked with 5% nonfat milk (dissolved in phosphate-buffered saline solution that contains 0.05% Tween 20 [PBST]) for 1 h, and probed with primary antibodies diluted in PBST with 1% nonfat milk at 4 °C overnight. The following primary antibodies were used at the stated dilution: mouse anti-rat CYP1A2 (sc-53241, Santa Cruz Biotechnology, Inc., 1:1000); rabbit anti-mouse Cyp2b10 mAb (AB9916, EMD Millipore, 1:5000); mouse anti-rat CYP3A1 mAb (sc-53246, Santa Cruz Biotechnology, Inc., 1:500); rat anti-mouse Mrp4 (M4I-10, University of Kansas Medical Center, 1:2000). The membranes were then incubated with a species-appropriate secondary antibody conjugated with horseradish peroxidase (HRP) (Sigma Aldrich, St. Louis, MO) diluted 1% nonfat milk in PBST. Protein bands were developed using a Novex® ECL Chemiluminescent Substrate Reagent Kit (Life Technologies, Carlsbad, CA). Membranes were stripped and re-incubated with primary antibodies for β-actin or histone H3 (Abcam, Cambridge, MA) as loading controls.

Enzyme activity quantifications

The crude membranes were prepared as described in the paragraph above. Enzyme activities for Cyp1a, Cyp2b and Cyp3a were quantified using the P450-Glo CYPA1, CYP2B, and CYP3A assay systems (Promega) following the manufacturer's protocol. Briefly, 20μg protein and a P450-Glo™ substrate (100 μM Luciferin-ME for Cyp1a, 3 μM Luciferin-2B6 for Cyp2b, and 3 μM IPA for Cyp3a) were combined in potassium phosphate (KPO4) buffer in 2 × concentrated mixture. The reaction was initiated by adding one volume of 2×concentrated NAPDH regenerating system (25 μl added for a final volume of 50 μl in an opaque 96-well plate). The products produced in the CYP reaction were detected as a luminescent signal from

DMD Fast Forward. Published on February 23, 2017 as DOI: 10.1124/dmd.117.075135
This article has not been copyedited and formatted. The final version may differ from this version.

a luciferase reaction using a Plate-lumino Biomedical system (Promega Corporation, Madison). Signals were allowed to stabilize for 20 minutes at room temperature before reading on a luminometer.

Serum ALT quantification

Serum samples from WT (Corn Oil, TCPOBOP), CAR-null (Corn Oil, TCPOBOP) and hCAR-TG (Corn Oil, CITCO) mice were analyzed by standard enzyme-colorimetric assays using a liquid ALT kit according to the manufacturer's protocol (Pointe Scientific, Canton, MI). The absorbance was quantified spectrophotometrically at wavelengths of 340 and 540 nm.

Statistical analysis

A total of 393 DPGs genes with known functions for xenobiotic biotransformation were retrieved from the Cufflinks output for further analysis. The genes that were expressed with an average FPKM > 1 in at least one group were considered to be significantly expressed in liver, and this criteria was selected based on the literature (Peng et al., 2016). Differential expression of the RNA-Seq data was considered at FDR-BH<0.05. Venn diagram was generated using the VennDiagram package in R utilizing the draw.quad.venn function. Heatmap was plotted using JMP (Ward method, standardized data, SAS, Cary, NC). For RT-qPCR and protein assays, two-way analysis of variance (ANOVA) was used for multiple group comparisons (IBM SPSS statistics 19, Armonk, NY) (Tukey's post-hoc test, $p<0.05$). Asterisks (*) represent significant difference between Corn Oil and TCPOBOP in Wild type mice. Dollar sign ($) represent significant difference between Corn Oil and TCPOBOP in CAR-null mice. Pounds (#) represent significant difference between Corn Oil and CITCO in hCAR-TG mice.

RESULTS

Regulation of mouse (m) and human (h) CAR signaling in developing livers of WT, CAR-null, and hCAR-TG mice

The animal dosing regimen is shown in Figure 1A. Because the dose-response of CAR ligands in adult mice and primary hepatocyte culture has been well established before (Honkakoski et al., 1992; Honkakoski and Negishi, 1998; Maglich et al., 2003; Scheer et al., 2008), a single optimal dose was selected at adult age in the present study. Because relatively less is known regarding the dose-response relationship of CAR activation and targeted DPG expression in newborns, a dose-response of TCPOBOP and CITCO was performed at 5-day-old neonatal age. Serum ALT levels were low in all treatment groups, except for a moderate increase in livers of WT mice at the medium dose of TCPOBOP. The highest average serum ALT value was 33.54 U/L, which was within the normal range (Supplemental Figure 1). To confirm the mouse genotypes and the regulation of CAR in liver by age and CAR ligands, RT-qPCR was performed in livers of WT, CAR-null, and hCAR-TG mice (Figure 1B). As expected, the mCAR mRNA was only detected in livers of WT mice but not in livers of CAR-null or hCAR-TG mice. During development, the mCAR mRNA increased from 5- to 60-days of age in livers of control WT mice. Interestingly, the mCAR ligand TCPOBOP at the highest dose markedly decreased the mCAR mRNA at both ages (Figure 1B and supplemental Figure 2A). These data suggest a negative feedback mechanism upon the pharmacological activation of CAR to reduce CAR-signaling at the transcription level. Regarding the regulation of the hCAR mRNA, the 5 hCAR splicing variants (SVs), namely SV0, SV1, SV2, SV3 and SV4 (Zhang et al., 2013; Lamba et al., 2004), were quantified as shown in Figure 1C. This nomenclature is the same as used in a pervious study (Jinno et al., 2004), in that SV0 refers to NM_005122; SV1 has an in-frame 12bp insertion; SV2 has an in-frame 15bp insertion; SV3 has both 12bp and 15bp insertions; whereas SV4 has an in-frame 117bp deletion. This nomenclature is slightly different from another study (Arnold et al., 2004), in that SV0 (present study) is termed SV3, SV3 (present study) is termed SV6 by Arnold et al., whereas SV2 and SV4 are the same for both papers. SV0 and SV2 were the major hCAR transcripts, followed by SV1 and SV3, which were expressed at lower levels, whereas SV4 was minimally expressed throughout liver

DMD Fast Forward. Published on February 23, 2017 as DOI: 10.1124/dmd.117.075135
This article has not been copyedited and formatted. The final version may differ from this version.

development. All 4 expressed transcripts (SV0-SV3) were increased from 5- to 60-days of age. Unlike mCAR, the hCAR ligand CITCO did not alter the expression of any hCAR splice variants at either age. The prototypical CAR-target gene Cyp2b10 was up-regulated by both mCAR and hCAR activation at Day 60 in a CAR-dependent manner; whereas at Day 5, Cyp2b10 was up-regulated by mCAR at all three doses of TCPOBOP in livers of WT mice, and by hCAR at the medium and high doses of CITCO in livers of hCAR-TG mice (Supplemental Figure 2B). In summary, these observations confirmed the 3 genotypes of mice, and demonstrated that both the mCAR and the hCAR transcripts were up-regulated from neonatal to adult age, however, only the mCAR ligand down-regulated the hepatic mCAR expression, whereas the hCAR ligand did not alter the expression of the hCAR transcripts at either developmental ages. In newborns, both mCAR and hCAR are functionally active and respond to chemical induction of target genes.

Regulation of hepatic DPGs by pharmacological activation of mCAR and hCAR during development.

To determine the effect of age, species, and pharmacological activation of CAR on the regulation of DPGs in liver, RNA-Seq was performed in livers of WT and hCAR-TG mice that were treated with vehicle or a species-appropriate CAR ligand at 5- and 60-days of age.

Previously, a dose-response of the mCAR ligand TCPOBOP and the hCAR ligand CITCO was established in adult mice and primary hepatocyte culture (Honkakoski et al., 1992; Honkakoski and Negishi, 1998; Maglich et al., 2003; Scheer et al., 2008), however, very little is known regarding the optimal dose range of CAR activation in newborns. Therefore, a dose-response of TCPOBOP and CITCO was performed at 5-day-old neonatal age in livers of WT, CAR-null, and hCAR-TG mice (Supplemental Figures 2-3). The mCAR mRNA was down-regulated, whereas the prototypical CAR-target gene Cyp2b10 was up-regulated by TCPOBOP at all doses in livers of WT mice at 5-days of age, in a CAR-dependent manner (Supplemental

Figure 2). Interestingly, at Day 5 neonatal age, many other DPGs were dose-dependently regulated by CAR activation. For example, the Phase-I enzymes Cyp1a2, Cyp3a11, Nqo1, and Aldh1a1, the Phase-II enzymes Ugt2b35, Gstm1, Gstm3, and Sult5a1, as well as efflux transporters Mrp3 and Mrp4 were all up-regulated by both mCAR and hCAR activation in a CAR-dependent manner (Supplemental Figure 3). Based on the dose-response studies on the DPG expression in WT and hCAR-TG mice at 5-days of age (Supplemental Figure 2-3), the highest doses were selected for RNA-Seq for both TCPOBOP- and CITCO-treated groups, whereas a single optimal dose was selected at 60-day-old adult age based on the literature.

RNA-Seq generated approximately 47 to 68 million reads per sample, among which approximately 40 to 60 million reads were uniquely mapped to the mouse reference genome (NCBI GRCm/38/mm10). As shown in Figure 2A, among all the 393 DPGs with known important functions in xenobiotic biotransformation (Supplemental Table 1) (Parkinson et al., 2013), 90 DPGs were not expressed in livers of any groups (threshold: average FPKM < 1 in all treatment groups); whereas a total of 303 genes were expressed in livers of at least one groups, among which 258 DPGs were differentially regulated by mCAR or hCAR activation in either Day 5 or Day 60 (FDR-BH<0.05), and 45 genes were stably expressed among all treatment groups.

A Venn diagram (Figure 2B) of the 258 differentially regulated DPGs displayed a clear separation by age and species of CAR (threshold: average FPKM>1 in at least one group; FDR-BH<0.05 in at least one comparison). Regarding age-specificity, between Day 5 WT (orange) and Day 60 WT (red), there were 144 DPGs commonly regulated by mCAR at both ages, whereas 44 DPGs were uniquely regulated by mCAR activation only at Day 5 neonatal age, and 64 DPGs were uniquely regulated by mCAR activation only at Day 60. Similarly, hCAR activation also displayed age-specificity, in that between Day 5 hCAR-TG (green) and Day 60 hCAR-TG (blue), there were 48 DPGs differentially regulated at both ages by hCAR activation,

DMD Fast Forward. Published on February 23, 2017 as DOI: 10.1124/dmd.117.075135
This article has not been copyedited and formatted. The final version may differ from this version.

whereas 40 DPGs were uniquely regulated by hCAR activation only at Day 5 neonatal age, and 54 DPGs were uniquely regulated by hCAR activation at Day 60 adult age.

Regarding species-specificity, at the same developmental age, mCAR and hCAR produced overlapping but not identical effects on the expression of DPGs (Figure 2B). At Day 5 neonatal age, 74 DPGs were differentially regulated by both mCAR and hCAR activation, whereas a lot more DPGs (114) were uniquely regulated only by mCAR, and much fewer DPGs (14) were uniquely regulated only by hCAR. A similar trend was observed at Day 60 adult age, in that 92 DPGs were differentially regulated by both mCAR and hCAR activation, whereas 116 were uniquely regulated only by mCAR, and much less DPGs (10) were uniquely regulated only by hCAR.

In summary, pharmacological activation of CAR displayed both age- and species-specificities in modulating the expression of DPGs in liver. Whereas age profoundly alters the CAR-targeted DPG profiles in both genotypes, mCAR appears to target a lot more DPGs than hCAR at both ages.

A two-way hierarchical clustering dendrogram of individual FPKMs of the 258 differentially regulated DPGs is shown in Figure 3A. As expected, samples within the same treatment group were clustered together. Age appeared to be a more predominant separation factor than other factors such as chemical treatment and genotypes, evidenced by the first two major branches splitting the two ages in the dendrogram. DPGs in the upper right corner were neonatal-enriched, whereas DPGs in the lower left corners were adult-enriched. At the same developmental age, mCAR activation generally resulted in greater alterations in the targeted DPG expression than hCAR activation, evidenced by the further separation between the WT Corn Oil group and the WT TCPOBOP group within the same age. The hCAR activation appeared to up-regulate more DPGs at Day 60 adult age as compared to Day 5 neonatal age.

DMD Fast Forward. Published on February 23, 2017 as DOI: 10.1124/dmd.117.075135
This article has not been copyedited and formatted. The final version may differ from this version.

To estimate the overall capacity of all DPGs in liver from the transcriptomic data, the cumulative FPKM values of the 258 differentially regulated DPGs were plotted as shown in Figure 3B (threshold: average FPKM>1 in at least one group; FDR-BH<0.05 in at least one comparison). Both mCAR and hCAR activation up-regulated the cumulative expression of DPGs at both Day 5 and Day 60, but the hCAR activation resulted in a much weaker fold-increase as compared to mCAR activation, and the hCAR activation in Day 5 produced an even weaker inducible effect than at Day 60. Regarding the regulation of specific categories of DPGs, in control livers of both genotypes, the cumulative mRNAs of all DPGs, Phase-I enzymes, Phase-II enzymes, uptake transporters and efflux transporters were all increased from 5- to 60-days of age. Following CAR activation, the cumulative expression of Phase-I, -II, and efflux transporters were all up-regulated by both mCAR and hCAR at both developmental ages, with mCAR producing greater mRNA fold increases than hCAR at both ages, whereas for hCAR activation, Day 60 was a more inducible age than Day 5. In contrast, the cumulative mRNAs of uptake transporters were not readily inducible by CAR at either age or genotype; mCAR activation down-regulated the cumulative mRNAs of uptake transporters at 60-days of age.

In summary, the majority of liver-expressed DPGs were differentially regulated by pharmacological activation of CAR in an age- and species-specific manner. In general, the DPGs in the Phase-I, Phase-II, and efflux transporters category were more responsive to CAR activation than uptake transporters, and although the mCAR activation increased the cumulative expression of enzymes and efflux transporters at both ages, the hCAR activation preferably up-regulated the cumulative expression of these genes in adult age.

DPGs that were common targets of mCAR and hCAR at both Day 5 and Day 60 developmental ages.

DMD Fast Forward. Published on February 23, 2017 as DOI: 10.1124/dmd.117.075135
This article has not been copyedited and formatted. The final version may differ from this version.

Among the 44 differentially regulated DPGs by both mCAR and hCAR activation at both ages, the DPGs (36 in total) that were altered at least 30% (average FPKM>1 in at least one group, FDR-BH<0.05 in all groups) are shown in Figure 4. All of these 36 DPGs were up-regulated by CAR activation across species and age, indicating that the effect of CAR on common DPG targets across species and development is inducible rather than suppressive. Many commonly regulated DPGs had a greater mRNA fold-increase in Day 5 neonatal age as compared to Day 60 adult age of the same genotype (as shaded in red in Table 1). Specifically, this "neonatal preference" was manifested by a greater fold-increase at Day 5 by both mCAR and hCAR activation for the mRNAs of P450s including Cyp1a2, 2b10, 2c29, 2c37, 2c50, 2c54, and 3a25, other Phase-I enzymes such as aldehyde dehydrogenases Aldh1a1 and Aldh1a7, the carboyesterase Ces1g, and the flavin containing monooxygenase Fmo5, the Phase-II enzymes glutathione *S*-transferase Gstt3 and sulfotransferase Sult5a1, as well as the basolateral efflux transporters Abcc3 (Mrp3) and Abcc4 (Mrp4), by both mCAR and hCAR activation (Figure 4 and Table 1) (threshold: [fold-increase at Day 5] – [fold-increase at Day 60] > 30%). In addition, mCAR activation resulted in a greater fold-increase at Day 5 in the mRNAs of the P450s Cyp2c55, 3a11, 3a13, and 4f15, Ces1d and Ces2a, epoxide hydrolase 1 (Ephx1), the glucuronidation enzymes Ugt2b35 and 2b36, the glutathione conjugation enzyme prostaglandin E synthase (Ptges), as well as the methyltransferase Inmt, as compared to Day 60 WT livers. The hCAR activation resulted in a moderately greater fold-increase at Day 5 in the mRNA of Sult1d1 as compared to Day 60 hCAR-TG livers. Although most commonly regulated DPGs were preferentially up-regulated in newborns, there were 7 DPGs (Por, Akr1b7, Sult1c2, Gsta2, Gstm1, Gstm2, and Gstm3) that were preferentially up-regulated by both mCAR and hCAR at Day 60 adult age, and 4 DPGs (Cyp2c55, Ces2a, Ephx1, and Ugt2b35) that were preferentially up-regulated by hCAR at Day 60 adult age (Table 1, shaded in yellow). The DPGs that are not shaded in colors were up-regulated by CAR ligands to a similar extent between Day 5 and Day 60 of the same genotype.

DMD Fast Forward. Published on February 23, 2017 as DOI: 10.1124/dmd.117.075135
This article has not been copyedited and formatted. The final version may differ from this version.

DPGs that were uniquely regulated by mCAR at Day 5 neonatal age.

Among the 30 DPGs uniquely regulated by mCAR at Day 5 neonatal age (Figure 2B), there were 21 DPGs for which the mRNAs were altered at least 30% and these genes are shown in Figure 5 as highlighted in red boxes (threshold: average FPKM>1 in at least one group, FDR-BH<0.05 only in Day 5 WT group and fold change above 30%, as highlighted in red boxes). These DPGs include the Phase-I P450 enzymes Cyp2d10 (67% increase) and Cyp2d22 (58% increase), other Phase-I enzymes Akr1a1 (49% increase), Akr7a5 (58%), Aldh7a1 (44% increase), Bche (53% decrease), Bphl (36% increase), Ces1a (70% increase), Dhrs3 (58% increase), Dhrs13 (51% increase), Epx (35% increase), Mocos (1.4-fold increase), Prdx2 (33% increase), Srd39u1 (37% increase), Phase-II glutathione conjugation enzymes Gstp2 (100% increase), Gstt2 (1.31-fold increase), and Mgst1 (31% increase), Phase-II amino acid conjugation enzymes Acsm1 (55% increase), Glyat (1.16-fold increase), and Sars (31% increase), as well as the basolateral uptake transporter Slco2b1 (Oatp2b1) (62% decrease, although the basal expression was very low). At Day 60 adult age in WT mice and at both developmental ages in hCAR-TG mice, these genes were not readily altered by CAR activation.

DPGs that were uniquely regulated by mCAR at Day 60 adult age.

Among the 42 DPGs uniquely regulated by mCAR at Day 60 of age (Figure 2B), there were 25 DPGs for which the mRNAs were altered at least 30% and these genes are shown in Figure 6 as highlighted in red boxes (threshold: average FPKM>1 in at least one group, FDR-BH<0.05 only in Day 60 WT group and fold change above 30%, as highlighted in red boxes). These DPGs include the Phase-I P450s Cyp2a22 (93% increase), Cyp2j6 (30% decrease), Cyp4a12b (52% decrease), Cyp4f16 (1.45-fold increase), Cyp4v3 (61% decrease), other Phase-I enzymes including Aoc2 (31% decrease), Ces2h (3.36-fold increase), Ces3b (71% decrease), Dhrs11 (38% decrease), Ephx2 (50% decrease), Fmo4 (2.13-fold increase), Gpx8 (82% increase), Prdx3 (82% increase), Sdr42e1 (51% decrease), Phase-II sulfotransferase Sult3a1 (185.20-fold

DMD Fast Forward. Published on February 23, 2017 as DOI: 10.1124/dmd.117.075135
This article has not been copyedited and formatted. The final version may differ from this version.

increase), glutathione transferases Gstk1 (36% decrease), Gstcd (73% increase), methyltransferases As3mt (40% increase), Comt (59% decrease), Hnmt (55% increase), acetyltransferases Nat6 (39% decrease) and Nat8 (58% decrease), amino acid conjugation enzyme Acm5 (33% decrease), fatty acid conjugation enzyme Lcat (42% decrease), and the basolateral uptake transporter Slco1b2 (Oatp1b2) (35% decrease).

DPGs that were uniquely regulated by hCAR at Day 5 or Day 60 developmental ages.

In comparison to mCAR, unique hCAR-targeted DPGs were fewer at both developmental ages (3 at Day 5 and 2 at Day 60) (Figure 2B). Specifically, as highlighted in red boxes, only Fmo1 (35% decrease), Maoa (30% decrease), and Nat2 (58% increase) mRNAs were uniquely regulated by hCAR activation at Day 5 neonatal age (Figure 7A) (average FPKM>1 in at least one group, FDR-BH<0.05, and fold change at least 30%), and only Ugt2b5 mRNA (38% increase) was uniquely regulated by hCAR activation at Day 60 adult age (Figure 7B).

Age affecting the CAR-mediated regulatory patterns of certain DPGs in liver.

Interestingly, in livers of WT mice, between Day 5 and Day 60, mCAR activation produced opposite effects in the regulation of certain DPGs including P450s (Cyp2c38, 2c40, 2c69, 2e1, 2f2, and 2j5), Adh7, Aox2, Ugt2a3, and Nnmt, as shown in Figure 8A (highlighted in red boxes). Specifically, these DPGs were all up-regulated by mCAR at Day 5 neonatal age, but were all down-regulated by mCAR activation in Day 60 adult age. Among these DPGs, Cyp2c40 and 2c69 were also down-regulated by hCAR activation in Day 60 adult age. Similarly, age also reversed the CAR-mediated regulatory patterns in livers of hCAR-TG mice (Figure 8B), in that Cyp4a14 and 4a32 mRNAs were both up-regulated by hCAR activation at Day 5 neonatal age, but were both down-regulated by hCAR activation at Day 60 adult age (highlighted in red boxes).

In summary, age was a critical modifying factor in the CAR-signaling and the subsequent regulatory patterns of DPGs in liver. In general, neonatal age provided a more permissive environment for up-regulation of DPGs commonly targeted by CAR of both the mouse and the human origins; however, unique age- and/or species-specific regulations of DPGs were also observed, and in certain scenarios, age completely reversed the CAR-mediated regulatory patterns of certain DPGs.

RT-qPCR confirmation of selected DPGs in livers of WT, CAR-null, and hCAR-TG mice

RT-qPCR was performed to validate selected DPGs targeted by CAR in livers of WT, CAR-null, and hCAR-TG mice. A shown in Figure 9, RT-qPCR not only confirmed the RNA-Seq data of the "universally regulated" DPGs by CAR activation (namely Cyp2b10, Cyp3a11, Ugt2b35, Gstm1, Gstm3, Mrp3 and Mrp4) (Figure 4) as well as Sult3a1 that was uniquely regulated in Day 60 WT livers (Figure 6), but also demonstrated that these differential regulations were CAR-dependent (data from CAR-null mice). In summary, RT-qPCR results confirmed the regulation of these DPGs by CAR in an age- and species-specific manner.

Protein expression and enzyme activities of selected CAR-targeted DPGs in liver

Western blot experiments were performed to determine protein expression of Cyp1a2, Cyp2b10, Cyp3a, as well as the basolateral efflux transporter Mrp4 (Figure 10) in livers of control and CAR ligands treated WT or hCAR-TG mice at Day 5 and Day 60 developmental ages. Cyp1a2 protein was up-regulated by CAR ligands in livers of both WT and hCAR-TG mice more prominently at 5-days of age (5-fold by TCPOBOP and 3.14-fold by CITCO respectively, Image J quantification [data not shown]). In contrast, although there was also an apparent increase in the Cyp1a2 protein by CAR ligands at Day 60, the fold increase was very moderate. As shown in Figure 10B, consistent with the protein data, Cyp1a enzyme activities were preferably increased by activation of CAR of both species in Day 5 neonatal age, but not in Day 60 adult age. Considering that Cyp1a2 mRNA was marked up-regulated at Day 60 adult

age (Figure 4), these observations suggest that there is a suppressive post-transcriptional mechanism to prevent the up-regulation of a functional protein. The Day 5 specific up-regulation of Cyp1a enzyme activity was CAR-dependent, in fact, in livers of 5-day-old CAR-null mice, there was even a constitutive decrease in the Cyp1a enzyme activity (Figure 10B).

CAR activation in livers of WT and hCAR-TG mice up-regulated protein expression of these Cyp2b10 and Cyp3a11 at both Day 5 and Day 60 ages, consistent with mRNA data (Figure 10A). The fold-induction of Cyp2b enzyme activity was most prominent by TCPOBOP and CITCO at the age of 5-day (16.92-fold and 8.26-fold respectively), followed by up-regulation at the age of 60-day (7.35-fold and 112% respectively) (Figure 10B). The Cyp3a activity was induced in TCPOBOP-treated mouse livers at the age of 5-day and 60-day (9.34-fold and 12.16-fold respectively), whereas this induction was observed in CITCO-treated group to a much lesser extent (Figure 10B).

The Mrp4 protein was up-regulated at Day 5 by TCPOBOP and to a lesser extent at Day 60 in livers of WT mice; however, in livers of hCAR-TG mice, Mrp4 protein was only up-regulated by CITCO at Day 60, but not at Day 5 (Figure 10A). To note, although the Mrp4 mRNA was up-regulated by CITCO at Day 60 hCAR-TG livers, both the basal and the induced levels of this gene were very low as compared to the neonatal age, suggesting that the apparent mRNA increase from low levels does not translate into biological significance.

DISCUSSION

Taken together, the present study utilized a transcriptomic approach to compare the age- and species-specificities of mCAR and hCAR in modulating the *in vivo* pharmacological regulation of drug metabolizing enzymes and transporters in livers of mice, and validated the necessity of CAR in regulating the expression of selected DPGs in livers of CAR-null mice. Three regulatory patterns have been identified: DPGs in Pattern-1 (up-regulated with age) and Pattern-2 (down-regulated with age) were predominantly regulated by age, whereas DPGs in

DMD Fast Forward. Published on February 23, 2017 as DOI: 10.1124/dmd.117.075135
This article has not been copyedited and formatted. The final version may differ from this version.

Pattern 3 were predominantly regulated by CAR activation. Results from the present study have also demonstrated that although several DPGs are up-regulated by CAR in both species and in both ages following ligand activation, there were also distinct age- and species-effects of CAR in modulating the expression of many other DPGs. These distinct effects can be summarized into the following four categories: 1) pharmacological activation of CAR has both inducible effects and suppressive effects in the expression of many DPGs; 2) both age and species differences may alter CAR-mediated regulatory patterns of certain DPGs; 3) the transcription of some DPGs only responds to a specific age or a specific species; and 4) pharmacological activation of CAR may alter expression of DPGs that are known to be prototypical targets of other important transcription factors in an age- and species-specific manner, indicating that there are age- and species-specific cross-talks between CAR and other receptor signaling pathways in liver.

During postnatal liver development, the maturation of DPGs is a pivotal factor contributing to the developmental regulation of metabolic drug clearance in children. Under basal conditions, previous studies have summarized the ontogenic gene expression profiles of some DPGs including Phase-I, Phase-II and transporters in mouse or rat liver by CAR pharmacological activation (Cheng et al., 2005; Alnouti and Klaassen, 2006; Alnouti and Klaassen, 2008; Cui et al., 2010; Cui et al., 2012a; Cui et al., 2012b; Peng et al., 2012; Peng et al., 2013; Pratt-Hyatt et al., 2013). Understanding the regulation of DPGs in newborns and children is important, so as to improve the safety and efficacy of using drugs in pediatric patients. However, relatively less is known regarding the inducibility of DPGs by chemical inducers in newborns. Because newborns are exposed to various types of xenobiotics, including therapeutic drugs and environmental toxicants, it is important to characterize the potential age-specific modulation of DPGs following xenobiotic exposure. The present study has filled this critical knowledge gap regarding CAR-targeted DPGs during development.

DMD Fast Forward. Published on February 23, 2017 as DOI: 10.1124/dmd.117.075135
This article has not been copyedited and formatted. The final version may differ from this version.

Because many CAR activators are frequently used as therapeutic drugs in pediatric patients, understanding the common and unique CAR-targeted DPGs during liver development is critical. For example, targeting CAR agonists has been suggested as one of the ultimate goals for the management and treatment of total parenteral nutrition cholestasis - common in infants (Hendaus, 2013). The traditional herbal medicine as Yin Zhi Huang from *Artemisia capillaris*, is a CAR activator that has been widely used in Asia to prevent and treat neonatal jaundice (Huang et al., 2004), which is a clinical disorder of reduced bile flow. The herbal extract of the *Phyllanthus amarus* root has been shown to decrease bilirubin and oxidative stress in drug-induced neonatal jaundice in mice, and this correlates with up-regulated hepatic CAR and Cyp3a expression that account for enhanced bilirubin clearance (Maity et al., 2013). Given the wide application of CAR activators in pediatric patients, the age-specific regulation of hepatic DPGs by CAR may serve as a major risk factor for adverse drug reactions in newborns and children, and may alter the pharmacokinetics of drugs and other environmental chemicals. For example, phenobarbital, an indirect CAR activator that has been used as an effective and safe anticonvulsant drug in infants with seizures, is primarily metabolized in liver by CYP2C9 in humans, and the half-life of this drug is longer in adults (100 hours) as compared to 4-week-old infants (67 hours) (Pacifici, 2016). Interestingly, the present study has shown that most of the differentially regulated Cyp2c family members were more induced in newborns than in adults by both mCAR and hCAR (Table 1). The greater inducibility of Cyp2c enzymes may at least in part explain the lower half-life of Cyp2c substrates (such as phenobarbital) in newborns. The persistent environmental toxicants polybrominated diphenyl ethers (PBDEs), which cause a wide spectrum of toxicities including neurodevelopmental disorders (Costa and Giordano, 2007; Hoffman et al., 2012), are detected in human breast milk in U.S. women at worrisome levels (Daniels et al., 2010). Several breast milk-enriched PBDE congeners have been shown to be primarily metabolized by the human CYP2B6 enzyme (Erratico et al., 2012; Gross et al., 2015), generating hydroxylated metabolites that are generally considered more toxic than the parent

DMD Fast Forward. Published on February 23, 2017 as DOI: 10.1124/dmd.117.075135
This article has not been copyedited and formatted. The final version may differ from this version.

compounds. The mouse homolog Cyp2b10 was up-regulated to a much greater extent in livers of both WT and hCAR-TG mice in newborns than in adults (Table 1), and this may in part explain why newborns are more vulnerable to PBDE-mediated toxicities than adults. Regarding the human CYP3A4, which is the most abundant hepatic Phase-I CYP enzyme that metabolizes approximately 50% marketed drugs (Zhou, 2008), the present study has shown that its mouse homolog Cyp3a11 is equally inducible by hCAR between newborns and adults, but is more inducible by mCAR between newborns and adults (Table 1). Although CYP3A4 is generally considered to be lowly expressed in human livers in newborns (Ince et al., 2013), the present study has suggested that, following xenobiotic exposure, the contribution of this enzyme in potential adverse drug reactions in pediatric patients should not be underestimated. In addition, it is also logical to predict that therapeutic drugs that are CAR activators may predispose the pediatric patients for environmental chemical induced toxicities by inducing certain DPGs.

Previously, a systematic study was conducted using multiplex suspension branched DNA amplification technology to evaluate the inducibility of various DPGs in livers of adult mice following CAR ligand TCPOBOP treatment (Aleksunes and Klaassen, 2012). In livers of adult WT mice, consistent with the previous study, all of the DPGs that were shown to be differentially regulated by TCPOBOP by Aleksunes et al. have also been shown to be differentially regulated in the same direction by CAR in the present study (supplemental Table 2) (Aleksunes and Klaassen, 2012). This includes the TCPOBOP-mediated up-regulation of the Phase-I enzymes Cyps (1a2, 2b10, 3a11) and Nqo1, Phase-II enzymes Gsts (a1, a4, m1, m3, m4, t1), Sults (1e1, 3a1, 5a1), Papss2, Ugts (1a1, 1a9, 2b34-36), and transporters Slco1a4, Abcc2-3, as well as the TCPOBOP-mediated down-regulation of Ugt2a3 and Slco1a1. The present study also demonstrated that most of these DPGs were hCAR targets at 60-days adult age, except for Nqo1, Sult3a1, Papss2, and Ugt2a3, for which the mRNAs remained unchanged in livers of adult hCAR-TG mice following CITCO treatment (supplemental Table 2). In newborns, although

DMD Fast Forward. Published on February 23, 2017 as DOI: 10.1124/dmd.117.075135
This article has not been copyedited and formatted. The final version may differ from this version.

most of these DPGs were still differentially regulated by TCPOBOP in livers of WT mice, four DPGs, namely Gsta1, Sult1e1, Sult3a1, and Slco1a1, were not readily regulated by TCPOBOP at Day 5, and many more CAR-targeted DPGs shown in the previous study (Aleksunes and Klaassen, 2012) were unresponsive to CITCO in livers of hCAR-TG mice at Day 5 (supplemental Table 2). In summary, although many DPGs are commonly regulated by CAR between newborns and adults and between mice and humans, age- and species-specificities do exist.

A study utilizing microarray profiling in livers of WT and CAR-null mice after exposure to various CAR activators have constructed a CAR-dependent biomarker signature following xenobiotic insult (Oshida et al., 2015). Specifically, there are 83 CAR-dependent genes identified by Oshida et al. from the two genotypes of mice following exposure to three structurally diverse CAR activators (CITCO, phenobarbital, and TCPOBOP). The present study has confirmed the *bona fide* CAR-target genes as compared to the previous study, such as Cyp2b10, Cyp2c55, Gstm1, Ugt2b34, Cyp1a2, Cyp4f15, and Aldh1a1.

Another recent study utilized wild-type and CAR-null HepaRG cells, which are human liver cancer-derived cell lines, to determine transcriptome-wide regulation of human CAR *in vitro*, and found that CITCO differentially regulated 135 genes whereas phenobarbital differentially regulated 133 genes in a hCAR-dependent manner (Li et al., 2015). Interestingly, compared to the hCAR-TG data in the present study (supplemental Table 2), many hCAR-targeted DPGs in HepaRG cells were also differentially regulated in hCAR knockout conditions following CITCO or phenobarbital treatment (Li et al., 2015). In addition, hCAR activation by CITCO differentially regulates many more DPGs in the present study than in HepaRG cells in the previous study. The differences in the observations indicate that CITCO may have certain off-target effects in modulating DPG expression in human hepatocytes; furthermore, the hCAR activation in mouse hepatocytes *in vivo* may differ from hCAR activation in human hepatocytes *in vitro*, likely due to

species differences in the enhancers of DPGs, and/or chromatin epigenetic differences between the two model systems. Future studies are needed to determine the epigenetic mechanisms of the age- and species-specificities of CAR in modulating DPGs in liver.

ACKNOWLEDGEMENTS

The authors would like to thank Dr. Debbie Nickerson's laboratory in UW Genome Science Department, and all members in the UW EDGE Functional Genomics & Proteomics Facility Core for their technical assistance in RNA sequencing. The authors also would like to thank the members of Dr. Cui laboratory for their help in tissue collection and proof-reading the manuscript.

AUTHORSHIP CONTRIBUTIONS

Participated in research design: Cheng and Cui

Conducted experiments: Cheng and Cui

Performed data analysis: Cheng, Bammler, and Cui

Wrote or contribute to the writing of the manuscript: Cheng, Bammler, and Cui

REFERENCES

Aleksunes LM and Klaassen CD (2012) Coordinated regulation of hepatic phase I and II drug-metabolizing genes and transporters using AhR-, CAR-, PXR-, PPARalpha-, and Nrf2-null mice. *Drug Metab Dispos* **40:**1366-1379.

Almazroo OA, Miah MK, and Venkataramanan R (2017) Drug metabolism in the liver. *Clin Liver Dis* **21**: 1-20.

Arnold KA, Eichelbaum M, and Burk O (2004) Alternative splicing affects the function and tissue-specific expresion of the human constitutive androstane receptor. *Nucl Recept* **2**(1): 1.

Alnouti Y and Klaassen CD (2006) Tissue distribution and ontogeny of sulfotransferase enzymes in mice. *Toxicol Sci* **93:**242-255.

Alnouti Y and Klaassen CD (2008) Tissue distribution, ontogeny, and regulation of aldehyde dehydrogenase (Aldh) enzymes mRNA by prototypical microsomal enzyme inducers in mice. *Toxicol Sci* **101:**51-64.

Bookout AL, Jeong Y, Downes M, Yu RT, Evans RM, and Mangelsdorf DJ (2006) Anatomical profiling of nuclear receptor expression reveals a hierarchical transcriptional network. *Cell* **126:**789-799.

Chakraborty S, Kanakasabai S, and Bright JJ (2011) Constitutive androstane receptor agonist CITCO inhibits growth and expansion of brain tumour stem cells. *Br J Cancer* **104:**448-459.

Chen WD, Fu X, Dong B, Wang YD, Shiah S, Moore DD, and Huang W (2012) Neonatal activation of the nuclear receptor CAR results in epigenetic memory and permanent change of drug metabolism in mouse liver. *Hepatology* **56:**1499-1509.

Cheng X, Maher J, Chen C, and Klaassen CD (2005) Tissue distribution and ontogeny of mouse organic anion transporting polypeptides (Oatps). *Drug Metab Dispos* **33:**1062-1073.

Costa LG and Giordano G (2007) Developmental neurotoxicity of polybrominated diphenyl ether (PBDE) flame retardants. *Neurotoxicology* **28:**1047-1067.

Cui JY, Choudhuri S, Knight TR, and Klaassen CD (2010) Genetic and epigenetic regulation and expression signatures of glutathione S-transferases in developing mouse liver. *Toxicol Sci* **116:**32-43.

Cui JY, Gunewardena SS, Yoo B, Liu J, Renaud HJ, Lu H, Zhong XB, and Klaassen CD (2012a) RNA-Seq reveals different mRNA abundance of transporters and their alternative transcript isoforms during liver development. *Toxicol Sci* **127:**592-608.

Cui JY and Klaassen CD (2016) RNA-Seq reveals common and unique PXR- and CAR-target gene signatures in the mouse liver transcriptome. *Biochim Biophys Acta* **1859:**1198-1217.

Cui JY, Renaud HJ, and Klaassen CD (2012b) Ontogeny of novel cytochrome P450 gene isoforms during postnatal liver maturation in mice. *Drug Metab Dispos* **40:**1226-1237.

Cui JY and Li CY (2016) Regulation of Xenobiotic Metabolism in the Liver. Comprehensive Toxicology, 3rd Edition, Chapter 9.05.

Daniels JL, Pan IJ, Jones R, Anderson S, Patterson DG, Jr., Needham LL, and Sjodin A (2010) Individual characteristics associated with PBDE levels in U.S. human milk samples. *Environ Health Perspect* **118:**155-160.

Erratico CA, Szeitz A, and Bandiera SM (2012) Oxidative metabolism of BDE-99 by human liver microsomes: predominant role of CYP2B6. *Toxicol Sci* **129:**280-292.

Fu ZD, Selwyn FP, Cui JY, and Klaassen CD (2016) RNA Sequencing Quantification of Xenobiotic-Processing Genes in Various Sections of the Intestine in Comparison to the Liver of Male Mice. *Drug Metab Dispos* **44:**842-856.

Gross MS, Butryn DM, McGarrigle BP, Aga DS, and Olson JR (2015) Primary role of cytochrome P450 2B6 in the oxidative metabolism of 2,2',4,4',6-pentabromodiphenyl ether (BDE-100) to hydroxylated BDEs. *Chem Res Toxicol* **28:**672-681.

Gunewardena SS, Yoo B, Peng L, Lu H, Zhong X, Klaassen CD, and Cui JY (2015) Deciphering the Developmental Dynamics of the Mouse Liver Transcriptome. *PLoS One* **10:**e0141220.

Hendaus M (2013) TPN cholestasis in infants: what do we know? Review. *Georgian Med News***:**32-39.

Hines RN (2007) Ontogeny of human hepatic cytochromes P450. *J Biochem Mol Toxicol* **21:**169-175.

Hines RN (2013) Developmental expression of drug metabolizing enzymes: impact on disposition in neonates and young children. *Int J Pharm* **452:**3-7.

Hines RN and McCarver DG (2002) The ontogeny of human drug-metabolizing enzymes: phase I oxidative enzymes. *J Pharmacol Exp Ther* **300:**355-360.

Hoffman K, Adgent M, Goldman BD, Sjodin A, and Daniels JL (2012) Lactational exposure to polybrominated diphenyl ethers and its relation to social and emotional development among toddlers. *Environ Health Perspect* **120:**1438-1442.

Holsapple MP, Pitot HC, Cohen SM, Boobis AR, Klaunig JE, Pastoor T, Dellarco VL, and Dragan YP (2006) Mode of action in relevance of rodent liver tumors to human cancer risk. *Toxicol Sci* **89:**51-56.

Honkakoski P, Auriola S, and Lang MA (1992) Distinct induction profiles of three phenobarbital-responsive mouse liver cytochrome P450 isozymes. *Biochem Pharmacol* **43:**2121-2128.

Honkakoski P and Negishi M (1998) Protein serine/threonine phosphatase inhibitors suppress phenobarbital-induced Cyp2b10 gene transcription in mouse primary hepatocytes. *Biochem J* **330 (Pt 2):**889-895.

Huang W, Zhang J, and Moore DD (2004) A traditional herbal medicine enhances bilirubin clearance by activating the nuclear receptor CAR. *J Clin Invest* **113:**137-143.

Huang W, Zhang J, Washington M, Liu J, Parant JM, Lozano G, and Moore DD (2005) Xenobiotic stress induces hepatomegaly and liver tumors via the nuclear receptor constitutive androstane receptor. *Mol Endocrinol* **19:**1646-1653.

Ince I, Knibbe CA, Danhof M, and de Wildt SN (2013) Developmental changes in the expression and function of cytochrome P450 3A isoforms: evidence from in vitro and in vivo investigations. *Clin Pharmacokinet* **52:**333-345.

Jinno H, Tanana-Kagawa T, Hanioka N, Ishida S, Saeki M, Soyama A, Itoda M, Nishimura T, Saito Y, Ozawa S, Ando M, and Sawada J (2004) Identification of novel alternative splice variants of human constitutive androstane receptor and characterization of their expression in the liver. *Mol Pharmacol* **65**: 496-502.

Klaassen CD and Aleksunes LM (2010) Xenobiotic, bile acid, and cholesterol transporters: function and regulation. *Pharmacol Rev* **62:**1-96.

Lamba JK, Lamba V, Yasuda K, Lin YS, Assem M, Thompson E, Strom S, and Schuetz E (2004) Expression of constitutive androstane receptor splice variants in human tissues and their functional consequences. *J Pharmacol Exp Ther* **311**: 811-821.

Lee JS, Ward WO, Wolf DC, Allen JW, Mills C, DeVito MJ, Corton JC (2008) Coordinated changes in xenobiotic metabolizing enzyme gene expression in aging male rats. *Toxicol Sci* **106**: 263-83.

Li CY, Cheng SL, Bammler TK, and Cui JY (2016a) Editor's Highlight: Neonatal Activation of the Xenobiotic-Sensors PXR and CAR Results in Acute and Persistent Down-regulation of PPARalpha-Signaling in Mouse Liver. *Toxicol Sci* **153:**282-302.

Li CY, Renaud HJ, Klaassen CD, and Cui JY (2016b) Age-Specific Regulation of Drug-Processing Genes in Mouse Liver by Ligands of Xenobiotic-Sensing Transcription Factors. *Drug Metab Dispos* **44:**1038-1049.

Li D, Mackowiak B, Brayman TG, Mitchell M, Zhang L, Huang SM, and Wang H (2015) Genome-wide analysis of human constitutive androstane receptor (CAR) transcriptome in wild-type and CAR-knockout HepaRG cells. *Biochem Pharmacol* **98:**190-202.

Lu H, Cui JY, Gunewardena S, Yoo B, Zhong XB, and Klaassen CD (2012) Hepatic ontogeny and tissue distribution of mRNAs of epigenetic modifiers in mice using RNA-sequencing. *Epigenetics* **7:**914-929.

Lu H, Gunewardena S, Cui JY, Yoo B, Zhong XB, and Klaassen CD (2013) RNA-sequencing quantification of hepatic ontogeny and tissue distribution of mRNAs of phase II enzymes in mice. *Drug Metab Dispos* **41:**844-857.

Maglich JM, Parks DJ, Moore LB, Collins JL, Goodwin B, Billin AN, Stoltz CA, Kliewer SA, Lambert MH, Willson TM, and Moore JT (2003) Identification of a novel human constitutive androstane receptor (CAR) agonist and its use in the identification of CAR target genes. *J Biol Chem* **278:**17277-17283.

Maity S, Nag N, Chatterjee S, Adhikari S, and Mazumder S (2013) Bilirubin clearance and antioxidant activities of ethanol extract of Phyllanthus amarus root in phenylhydrazine-induced neonatal jaundice in mice. *J Physiol Biochem* **69:**467-476.

McCarver DG and Hines RN (2002) The ontogeny of human drug-metabolizing enzymes: phase II conjugation enzymes and regulatory mechanisms. *J Pharmacol Exp Ther* **300:**361-366.

Mooij MG, Schwarz UI, de Koning BA, Leeder JS, Gaedigk R, Samsom JN, Spaans E, van Goudoever JB, Tibboel D, Kim RB, and de Wildt SN (2014) Ontogeny of human hepatic and intestinal transporter gene expression during childhood: age matters. *Drug Metab Dispos* **42:**1268-1274.

Mooij MG, van de Steeg E, van Rosmalen J, Windster JD, de Koning BA, Vaes WH, van Groen BD, Tibboel D, Wortelboer HM, and de Wildt SN (2016) Proteomic Analysis of the Developmental Trajectory of Human Hepatic Membrane Transporter Proteins in the First Three Months of Life. *Drug Metab Dispos* **44:**1005-1013.

O'Sullivan JL, Haedicke GJ, and Bevivino J (1989) Spontaneous postpartum factor VIII inhibitor development with bleeding into the face and neck. *Plast Reconstr Surg* **84:**802-805.

Oshida K, Vasani N, Jones C, Moore T, Hester S, Nesnow S, Auerbach S, Geter DR, Aleksunes LM, Thomas RS, Applegate D, Klaassen CD, Corton JC (2015) Identification of chemical modulators of the constitutive activated receptor (CAR) in a gene expression compendium. *Nucl Recept Signal* 13:e002. doi: 10.1621/nrs.13002.

Pacifici GM (2016) Clinical Pharmacology of Phenobarbital in Neonates: Effects, Metabolism and Pharmacokinetics. *Curr Pediatr Rev* **12:**48-54.

Parkinson A OB, Buckley DB, Kazmi F, Czerwinski M, and Parkinson O (2013) Biotransformation of Xenobiotics, in: *Casarett and Doull's toxicology : the basic science of poisons* (Casarett LJ, Doull J, and Klaassen CD eds), pp xv, 1310 p., 1311 leaf of plates, McGraw-Hill, New York.

Peng L, Cui JY, Yoo B, Gunewardena SS, Lu H, Klaassen CD, and Zhong XB (2013) RNA-sequencing quantification of hepatic ontogeny of phase-I enzymes in mice. *Drug Metab Dispos* **41:**2175-2186.

Peng L, Yoo B, Gunewardena SS, Lu H, Klaassen CD, and Zhong XB (2012) RNA sequencing reveals dynamic changes of mRNA abundance of cytochromes P450 and their alternative transcripts during mouse liver development. *Drug Metab Dispos* **40:**1198-1209.

Peng L, Piekos S, Guo GL, Zhong XB (2016) Role of farnesoid X receptor in establishment of ontogeny of phase-I drug metabolizing enzyme genes in mouse liver. Acta Pharm Sin B. **6**: 453-459.

Pratt-Hyatt M, Lickteig AJ, and Klaassen CD (2013) Tissue distribution, ontogeny, and chemical induction of aldo-keto reductases in mice. *Drug Metab Dispos* **41:**1480-1487.

Ross J, Plummer SM, Rode A, Scheer N, Bower CC, Vogel O, Henderson CJ, Wolf CR, and Elcombe CR (2010) Human constitutive androstane receptor (CAR) and pregnane X receptor (PXR) support the hypertrophic but not the hyperplastic response to the murine nongenotoxic hepatocarcinogens phenobarbital and chlordane in vivo. *Toxicol Sci* **116:**452-466.

Scheer N, Ross J, Rode A, Zevnik B, Niehaves S, Faust N, and Wolf CR (2008) A novel panel of mouse models to evaluate the role of human pregnane X receptor and constitutive androstane receptor in drug response. *J Clin Invest* **118:**3228-3239.

Sueyoshi T, Li L, Wang H, Moore R, Kodavanti PR, Lehmler HJ, Negishi M, and Birnbaum LS (2014) Flame retardant BDE-47 effectively activates nuclear receptor CAR in human primary hepatocytes. *Toxicol Sci* **137:**292-302.

Thomson MM, Hines RN, Schuetz EG, and Meibohm B (2016) Expression Patterns of Organic Anion Transporting Polypeptides 1B1 and 1B3 Protein in Human Pediatric Liver. *Drug Metab Dispos* **44:**999-1004.

Tzameli I, Pissios P, Schuetz EG, and Moore DD (2000) The xenobiotic compound 1,4-bis[2-(3,5-dichloropyridyloxy)]benzene is an agonist ligand for the nuclear receptor CAR. *Mol Cell Biol* **20:**2951-2958.

Windshugel B and Poso A (2011) Constitutive activity and ligand-dependent activation of the nuclear receptor CAR-insights from molecular dynamics simulations. *J Mol Recognit* **24:**875-882.

Wortham M, Czerwinski M, He L, Parkinson A, and Wan YJ (2007) Expression of constitutive androstane receptor, hepatic nuclear factor 4 alpha, and P450 oxidoreductase genes determines interindividual variability in basal expression and activity of a broad scope of xenobiotic metabolism genes in the human liver. *Drug Metab Dispos* **35:**1700-1710.

Xiao D, Chen YT, Yang D, and Yan B (2012) Age-related inducibility of carboxylesterases by the antiepileptic agent phenobarbital and implications in drug metabolism and lipid accumulation. *Biochem Pharmacol* **84**: 232-9.

Yamamoto Y, Moore R, Goldsworthy TL, Negishi M, and Maronpot RR (2004) The orphan nuclear receptor constitutive active/androstane receptor is essential for liver tumor promotion by phenobarbital in mice. *Cancer Res* **64:**7197-7200.

Yan J and Xie W (2016) A brief history of the discovery of PXR and CAR as xenobiotic receptors. *Acta Pharm Sin B* **6:**450-452.

Yang H and Wang H (2014) Signaling control of the constitutive androstane receptor (CAR). *Protein Cell* **5:**113-123.

Zhang XJ, Shi Z, Lyv JX, He X, Englert NA, and Zhang SY (2015) Pyrene is a Novel Constitutive Androstane Receptor (CAR) Activator and Causes Hepatotoxicity by CAR. *Toxicol Sci* **147:**436-445.

Zhang YK, Lu H, and Klaassen CD (2013) Expression of human CAR splicing variants in BAC-transgenic mice. *Toxicol Sci* **132:**142-150.

Zhou SF (2008) Drugs behave as substrates, inhibitors and inducers of human cytochrome P450 3A4. *Curr Drug Metab* **9:**310-322.

FOOTNOTES

This work was supported by National Institute of Health R01 grants [ES025708, GM111381 and ES019487], the University of Washington Interdisciplinary Center for Exposures, Diseases, Genomics & Environment [P30 ES007033], as well as the UW DEOHS Murphy Endowment**.**

FIGURE LEGENDS

Figure 1. A. The animal-dosing regimen: WT, CAR-null and hCAR-TG mice at two developmental ages were administered vehicle (corn oil, 10ml/kg, i.p.) or a species-appropriate CAR-ligand (i.p.) once daily for 4 consecutive days. Specifically, at 5-day-old neonatal age, WT and CAR-null mice were daily-administered corn oil or the mCAR ligand TCPOBOP at one of the three doses: 0.3,1 and 3 mg/kg; whereas hCAR-TG mice were daily-administered corn oil or the hCAR ligand CITCO at one of the three doses: 2.5, 10 and 30 mg/kg. At 60-day-old adult age, WT (n=5 per group) and CAR-null mice (n=4 per group) were daily-administered corn oil or TCPOBOP (3mg/kg); whereas hCAR-TG mice (n=5 per group) were daily-administered corn oil or CITCO (30mg/kg). **B**. Messenger RNA expression of mCAR in livers of control and chemical-treated mice of the three genotypes at the two developmental ages. **C.** Expression of various human CAR splice variants (SVs) in livers of vehicle and CITCO-treated hCAR-TG mice at Day 5 and Day 60. Data were generated by RT-qPCR, and are expressed as mean % of the housekeeping gene β-actin ± standard error of mean (S.E.M). Asterisks (*) indicate statistically significant differences as compared to vehicle-treated groups of the same age in WT mice.

Figure 2. RNA-Seq was conducted in livers of control and CAR-ligand treated male WT and hCAR-TG mice at Day 5 and Day 60 of age (n=3 per group). **A.** A pie chart showing DPGs that are not expressed in any groups (red), stably expressed in all groups (blue), and differentially expressed by CAR ligand in at least one of the four comparisons (i.e. Day 5 WT vehicle vs. Day 5 WT TCPOBOP; Day 60 WT vehicle vs. Day 60 WT TCPOBOP; Day 5 hCAR-TG vehicle vs. Day 5 hCAR-TG CITCO; Day 60 hCAR-TG vehicle vs. Day 60 hCAR-TG CITCO, FDR-BH < 0.05). **B.** A Venn diagram showing the commonly and uniquely regulated DPGs among the four comparisons as described in Figure 2A. Venn diagram was generated using the VennDiagram package in R utilizing the draw.quad.venn function.

DMD Fast Forward. Published on February 23, 2017 as DOI: 10.1124/dmd.117.075135
This article has not been copyedited and formatted. The final version may differ from this version.

Figure 3. A. A two-way hierarchical clustering dendrogram of all 258 differentially regulated DPGs by pharmacological activation of CAR in livers of WT and hCAR-TG mice at Day 5 and Day 60 of age (FDR-BH<0.05) (JMP v12.0, SAS, Cary, NC, using the Ward method and standardized data option). Each row represents an individual mouse with FPKM values of all differentially regulated DPGs in the liver, whereas each column shows the mRNA expression of an individual DPG among all the mice. Red represents relatively high expression, blue represents relatively low expression. **B.** Cumulative FPKM of differentially regulated DPGs, Phase-I enzymes, Phase-II enzymes, uptake transporters, and efflux transporters in livers of control and CAR-ligand-treated WT and hCAR-TG mice at Day 5 and Day 60 of age. Individual FPKM values of genes of the same category were added together within the same treatment group, and results are expressed as mean FPKM ± S.E.M. of three individual biological replicates per group. Asterisks (*) indicate statistically significant differences as compared to vehicle-treated groups of the same age in WT mice; pounds (#) indicate statistically significant differences as compared to vehicle-treated groups of the same age in hCAR-TG mice.

Figure 4. DPGs that were commonly regulated by both mCAR and hCAR and at both developmental ages (FDR-BH < 0.05, and with at least a 30% increase or decrease in mRNA expression). There are three individual biological replicates per group. Asterisks (*) indicate statistically significant differences as compared to vehicle-treated groups of the same age in WT mice; pounds (#) indicate statistically significant differences as compared to vehicle-treated groups of the same age in hCAR-TG mice.

Figure 5. DPGs that were differentially regulated only by mCAR activation at Day 5 (FDR-BH < 0.05, and with at least a 30% increase or decrease in mRNA expression). There are three individual biological replicates per group. Asterisks (*) indicate statistically significant differences as compared to vehicle-treated groups of the same age in WT mice.

Figure 6. DPGs that were differentially regulated only by mCAR activation at Day 60 (FDR-BH < 0.05, and with at least a 30% increase or decrease in mRNA expression). There are three individual biological replicates per group. Asterisks (*) indicate statistically significant differences as compared to vehicle-treated groups of the same age in WT mice.

Figure 7. DPGs that were differentially regulated only by hCAR activation at Day 5 (**A**) and at Day 60 (**B**) (FDR-BH < 0.05, and with at least a 30% increase or decrease in mRNA expression). There are three individual biological replicates per group. Pounds (#) indicate statistically significant differences as compared to vehicle-treated groups of the same age in hCAR-TG mice.

Figure 8. Age specificity in CAR-mediated regulation of DPGs in WT (**A**) and hCAR-TG (**B**) mice. The CAR-mediated regulatory patterns between Day 5 and Day 60 were opposite in livers of the same genotype (FDR-BH < 0.05). There are three individual biological replicates per group. Data are shown as mean FPKM ± S.E.M. Asterisks (*) indicate statistically significant differences as compared to vehicle-treated groups in WT mice. Pounds (#) indicate statistically significant differences as compared to vehicle-treated groups in hCAR-TG mice.

Figure 9. Validation of selected DPGs in livers of WT, CAR-null and hCAR-TG mice treated with corn oil or a species appropriate CAR ligand using RT-qPCR (n=5 biological replicates per group). Data were normalized to the expression of the housekeeping gene β-actin and are presented as mean ± S.E.M. Asterisks (*) indicate statistically significant differences as compared to vehicle-treated groups of the same age in WT mice. Pounds (#) indicate statistically significant differences as compared to vehicle-treated groups of the same age in hCAR-TG mice.

Figure 10. **A.** Western blotting analysis of the proteins of Cyp1a2, Cyp2b10, Cyp3a, Mrp4, and histone H3 (loading control) in livers of WT and hCAR-TG mice treated with corn oil or a

species-appropriate CAR ligand at Day 5 (top) and Day 60 (bottom). Due to space limit on the gel, 2 representative control samples were loaded, whereas 3 CAR-ligand treated samples were loaded. **B.** Enzyme activities of Cyp1a, Cyp2b, and Cyp3a in crude membranes of livers from WT, CAR-null, and hCAR-TG mice treated with corn oil or a species-appropriate CAR-ligand (n=5 per group). The Promega P450-Glo enzyme activity assay systems were used as described in MATERIALS AND METHODS. Data are presented as mean ± S.E.M. Asterisks (*) indicate statistically significant differences as compared to vehicle-treated groups of the same age in WT mice. Dollar signs ($) indicate statistically significant differences as compared to vehicle-treated groups of the same age in CAR-null mice. Pounds (#) indicate statistically significant differences as compared to vehicle-treated groups of the same age in hCAR-TG mice.

DMD Fast Forward. Published on February 23, 2017 as DOI: 10.1124/dmd.117.075135
This article has not been copyedited and formatted. The final version may differ from this version.

Table 1. DPGs that were commonly regulated by both mCAR and hCAR activation and at both developmental ages

(Data are expressed as ratios of the FPKM in CAR-ligand treated group over FPKM in vehicle-treated group of the same age and genotype)

Gene Symbols	WT (TCPOBOP/Corn Oil)		hCAR-TG (CITCO/Corn Oil)	
Age (Days)	Day 5	Day 60	Day 5	Day 60
Cyp1a2	5.72	2.90	6.48	1.99
Cyp2b10	397.45	201.52	154.93	5.44
Cyp2c29	215.63	6.98	73.99	1.83
Cyp2c37	7.98	4.09	4.37	2.16
Cyp2c50	33.58	4.74	22.84	2.07
Cyp2c54	35.16	4.66	20.73	2.04
Cyp2c55	284.18	124.01	7.98	14.05
Cyp3a11	9.48	4.03	4.24	4.00
Cyp3a13	5.24	2.44	1.48	1.70
Cyp3a25	2.67	1.39	2.09	1.33
Cyp4f15	3.14	1.89	1.50	1.42
Por	4.34	6.46	1.64	4.42
Akr1b7	5.93	371.33	1.45	17.68
Akr1c14	1.62	1.35	1.80	1.53
Aldh1a1	23.59	2.80	5.96	1.76
Aldh1a7	57.03	5.77	7.37	1.84
Ces1d	2.04	1.50	1.51	1.85
Ces1g	4.55	1.44	4.17	1.70
Ces2a	18.97	12.18	2.94	3.59
Ephx1	6.37	5.00	1.97	2.78
Fmo5	5.53	4.07	1.84	1.39
Ugt2b34	3.50	3.39	1.52	1.77
Ugt2b35	3.45	3.08	1.85	2.18
Ugt2b36	3.66	1.94	1.53	1.56
Sult1c2	3.59	13.44	1.57	3.28
Sult1d1	2.54	2.87	2.00	1.68
Sult5a1	10.98	1.63	1.86	1.40
Gsta2	7.09	8.54	4.72	5.09
Gstm1	12.39	12.74	2.05	4.81
Gstm2	8.01	23.52	1.50	2.40
Gstm3	127.97	192.51	3.09	16.06
Gstt3	43.17	8.47	6.79	3.09
Ptges	53.61	42.97	3.74	4.12
Inmt	6.71	2.12	1.65	2.38
Abcc3	16.53	3.62	2.56	2.22
Abcc4	21.09	16.46	3.68	2.65

DMD Fast Forward. Published on February 23, 2017 as DOI: 10.1124/dmd.117.075135
This article has not been copyedited and formatted. The final version may differ from this version.

Figure 1

A. Animal dosing regimen

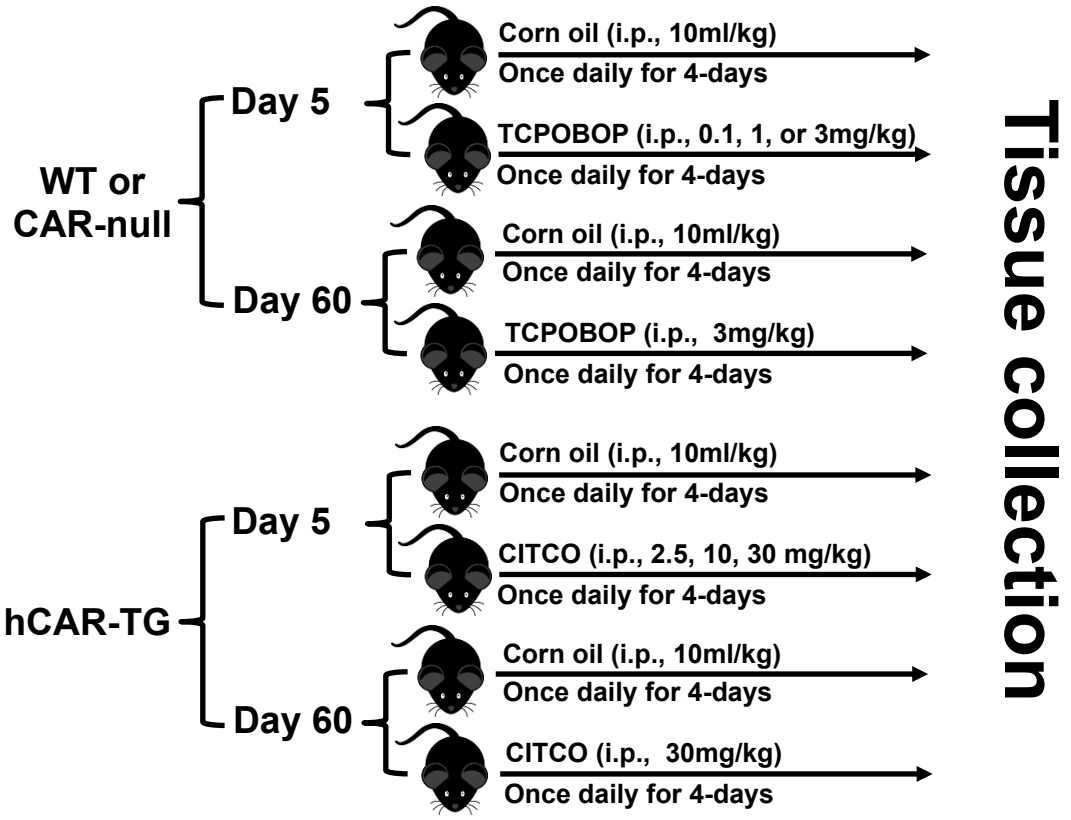

B. mCAR expression in the 3 genotypes

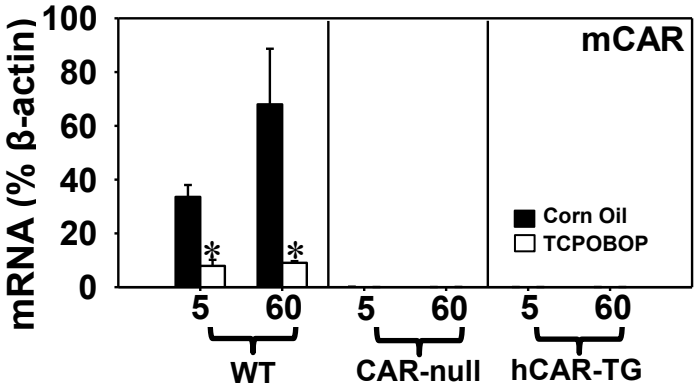

C. hCAR transcripts in hCAR-TG mice

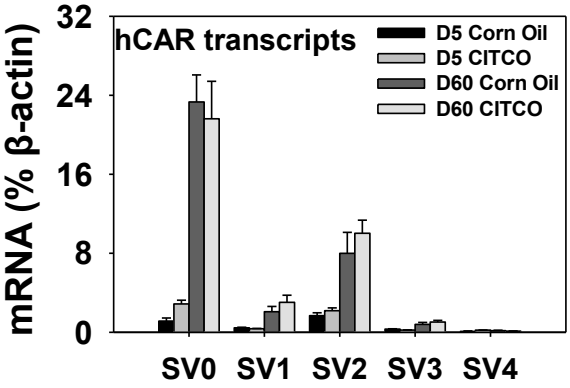

DMD Fast Forward. Published on February 23, 2017 as DOI: 10.1124/dmd.117.075135
This article has not been copyedited and formatted. The final version may differ from this version.

Figure 2

A

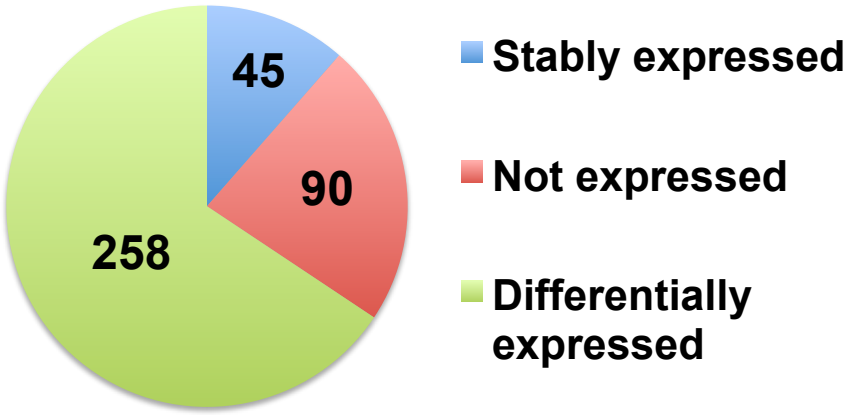

B

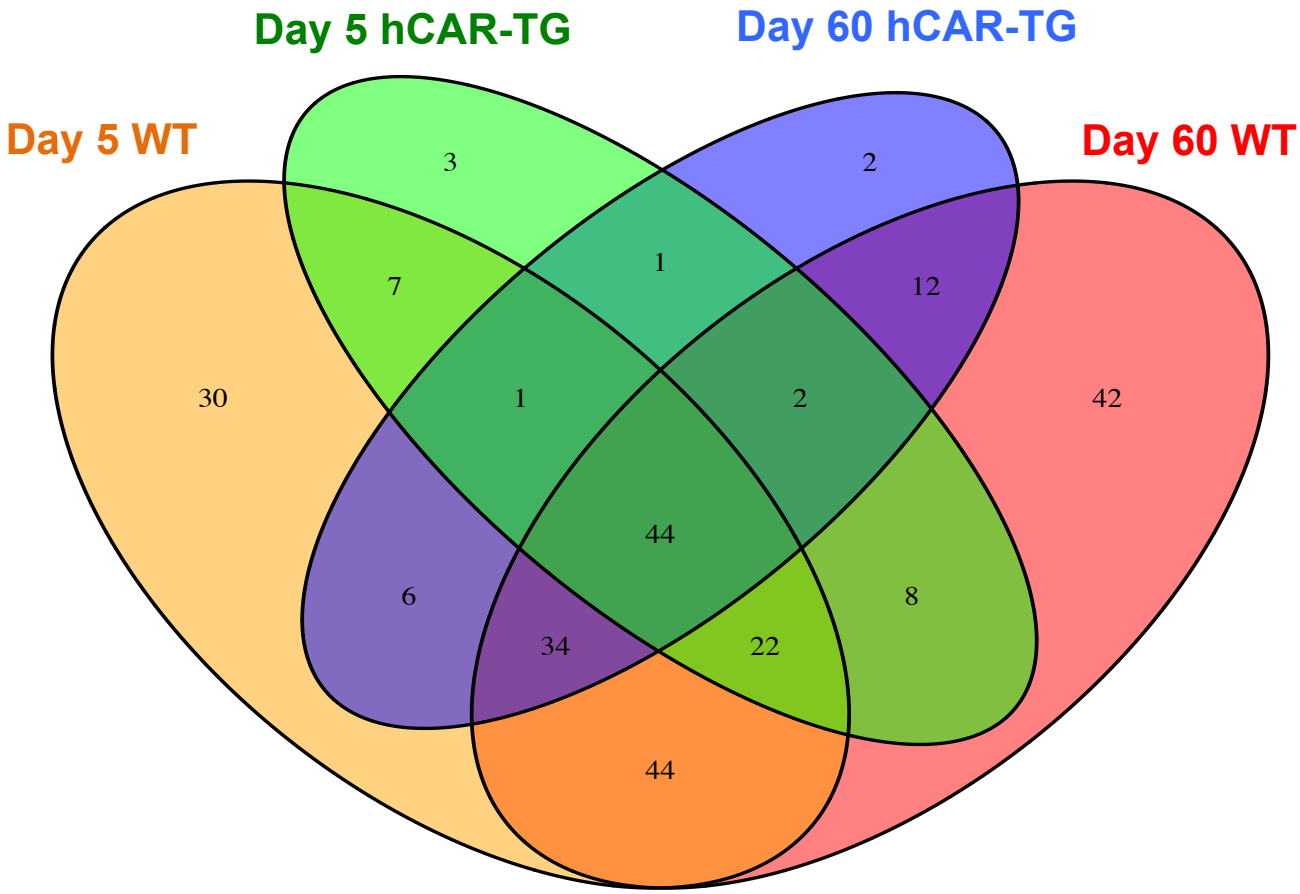

DMD Fast Forward. Published on February 23, 2017 as DOI: 10.1124/dmd.117.075135
This article has not been copyedited and formatted. The final version may differ from this version.

Figure 3

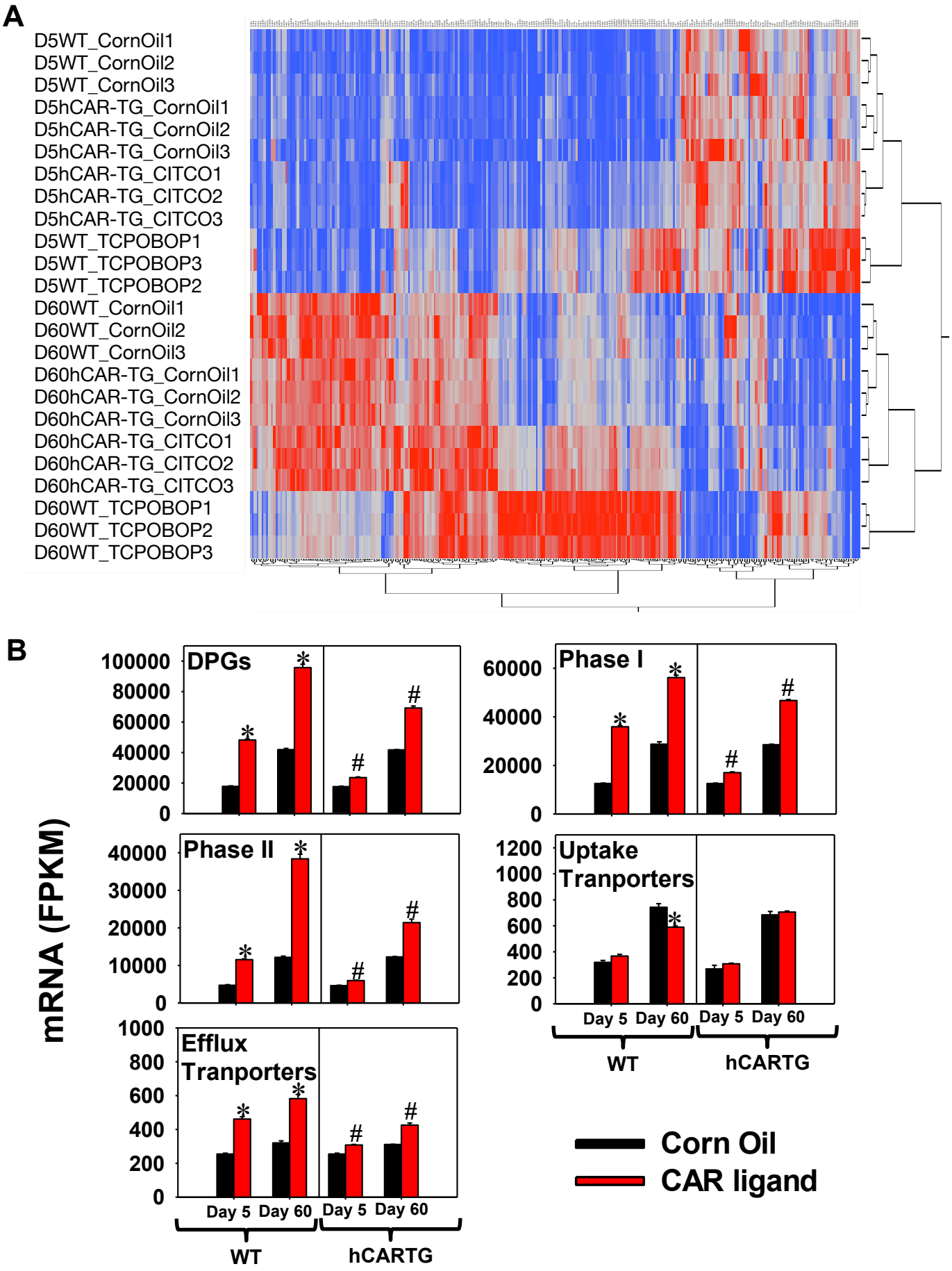

DMD Fast Forward. Published on February 23, 2017 as DOI: 10.1124/dmd.117.075135
This article has not been copyedited and formatted. The final version may differ from this version.

Figure 4

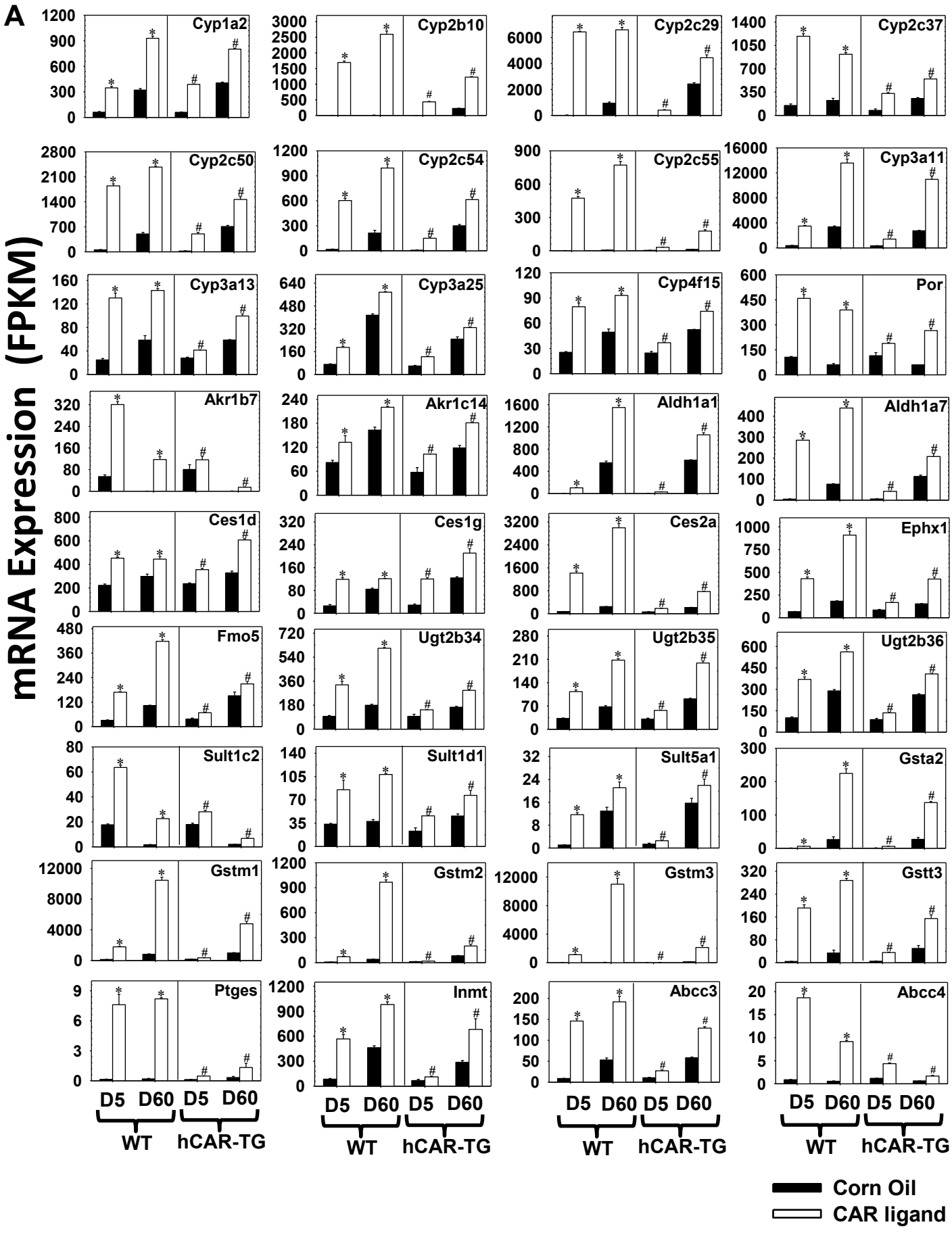

DMD Fast Forward. Published on February 23, 2017 as DOI: 10.1124/dmd.117.075135
This article has not been copyedited and formatted. The final version may differ from this version.

Figure 5

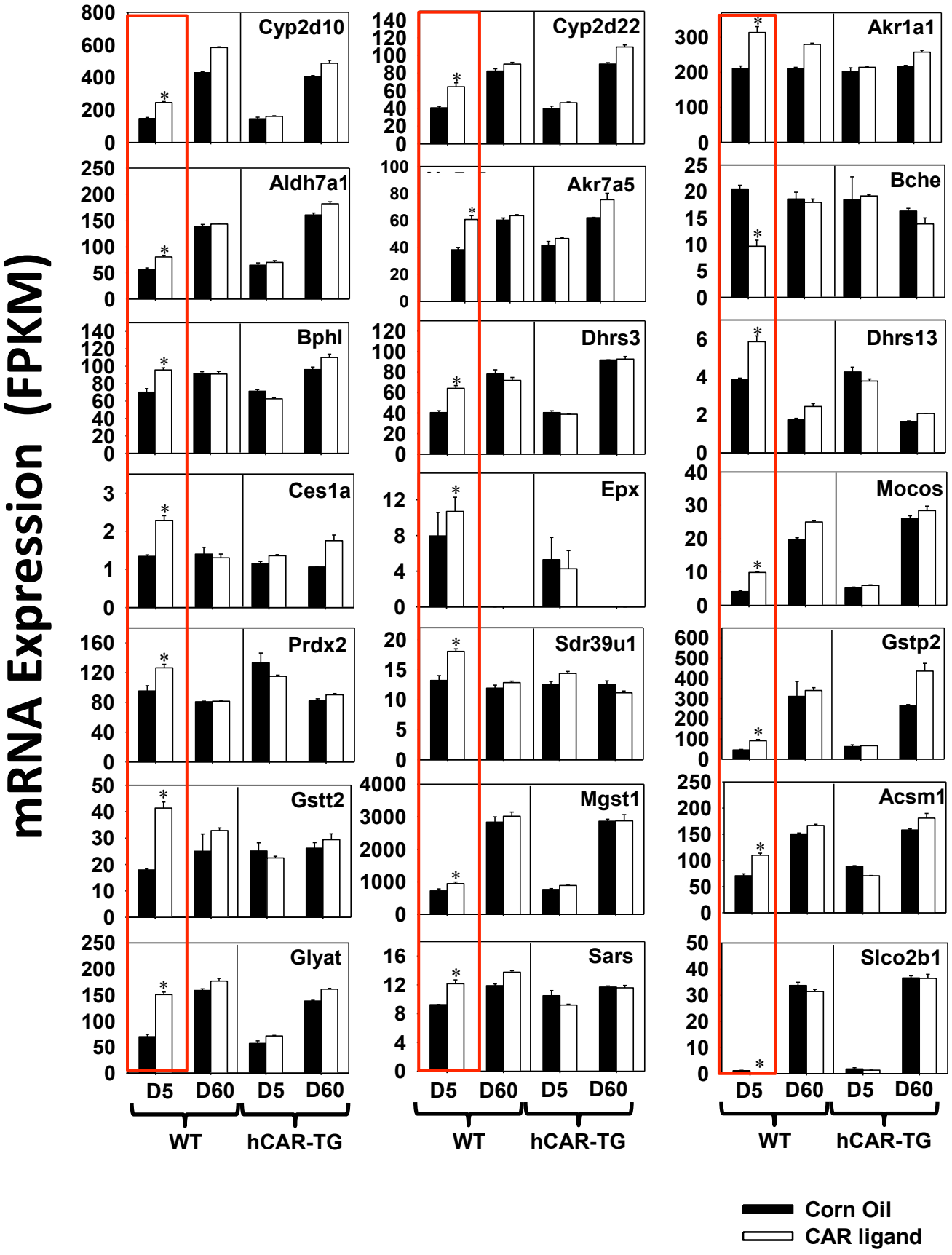

DMD Fast Forward. Published on February 23, 2017 as DOI: 10.1124/dmd.117.075135
This article has not been copyedited and formatted. The final version may differ from this version.

Figure 6

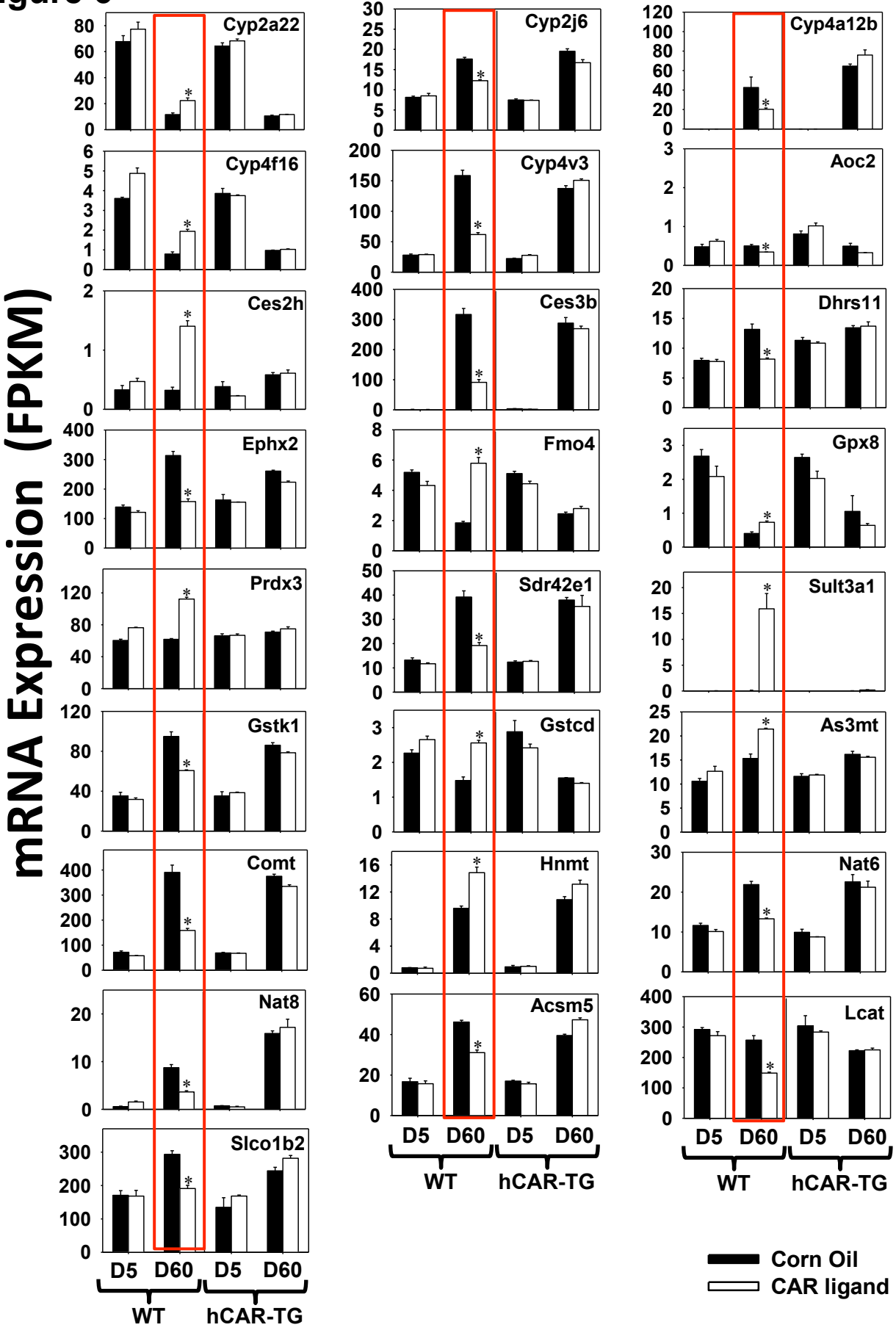

DMD Fast Forward. Published on February 23, 2017 as DOI: 10.1124/dmd.117.075135
This article has not been copyedited and formatted. The final version may differ from this version.

Figure 7

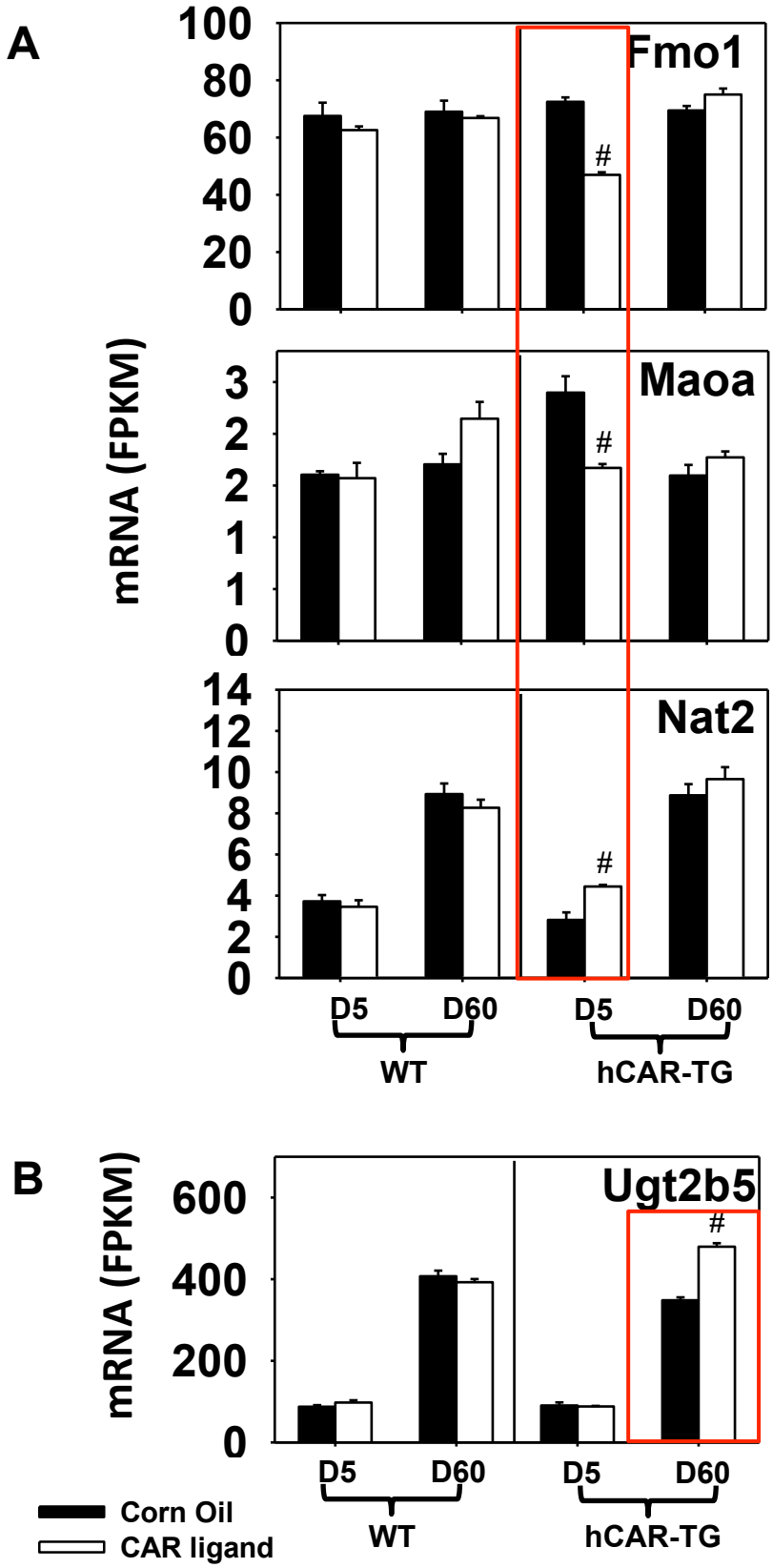

DMD Fast Forward. Published on February 23, 2017 as DOI: 10.1124/dmd.117.075135
This article has not been copyedited and formatted. The final version may differ from this version.

Figure 8

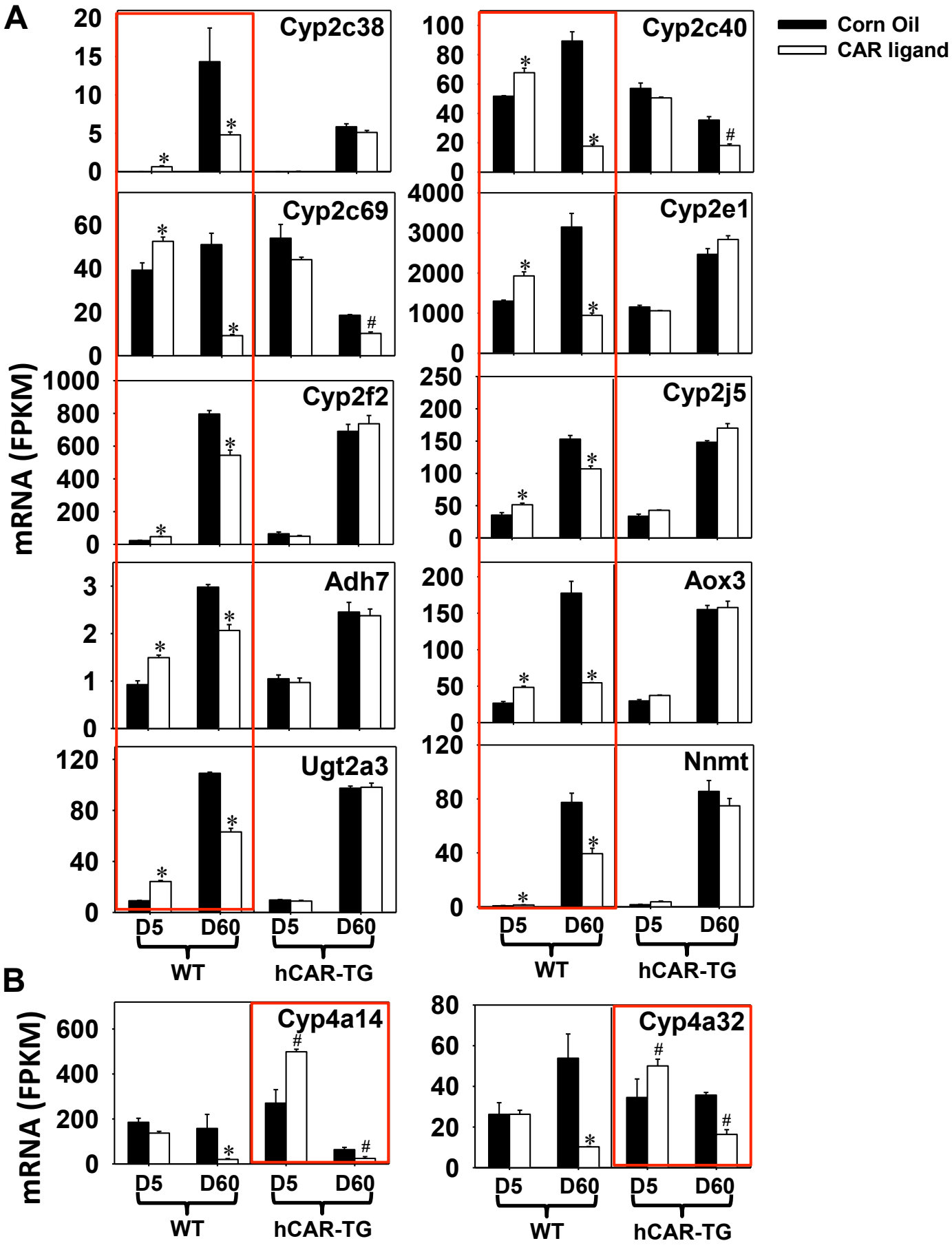

DMD Fast Forward. Published on February 23, 2017 as DOI: 10.1124/dmd.117.075135
This article has not been copyedited and formatted. The final version may differ from this version.

Figure 9

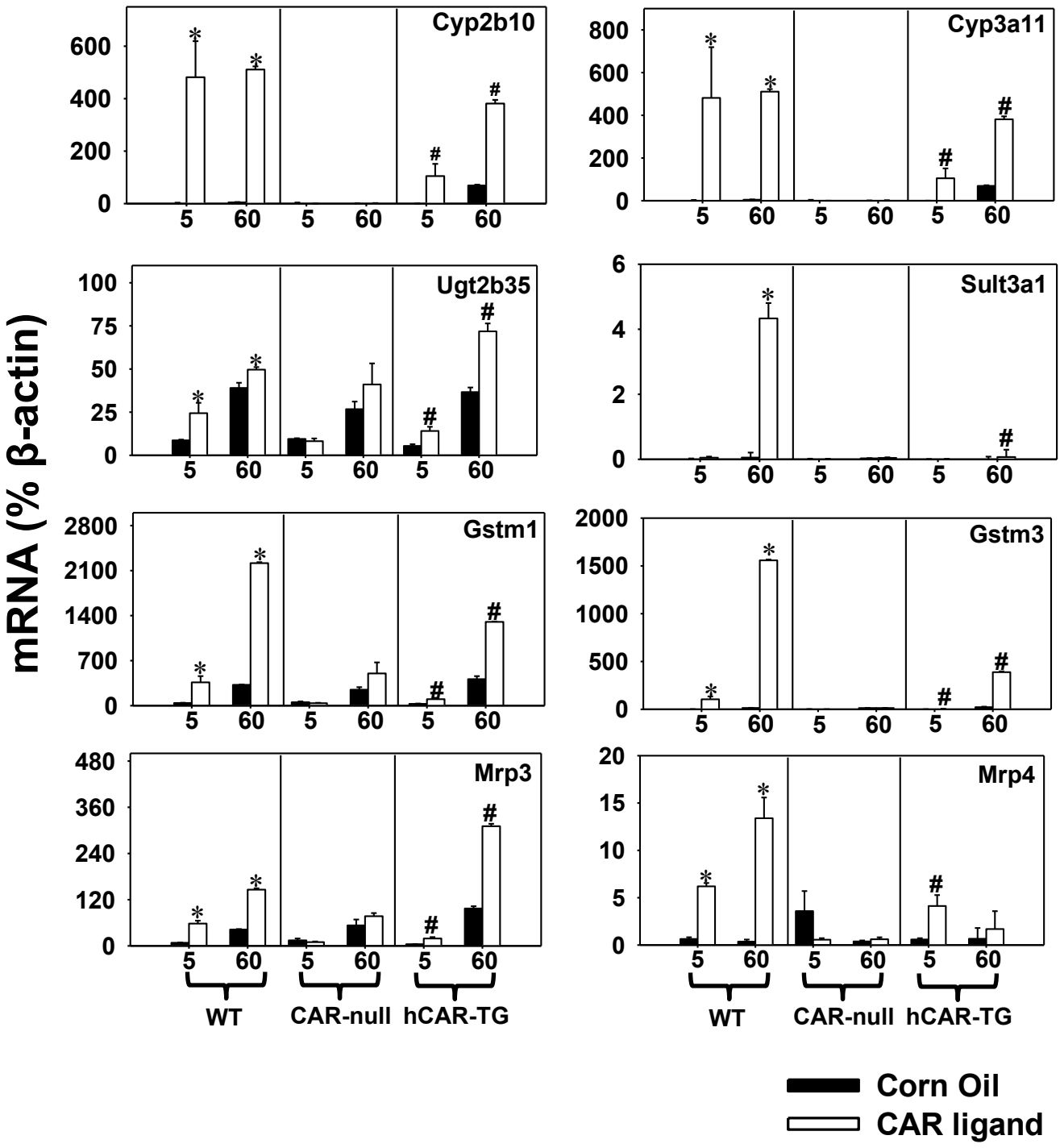

DMD Fast Forward. Published on February 23, 2017 as DOI: 10.1124/dmd.117.075135
This article has not been copyedited and formatted. The final version may differ from this version.

Figure 10